

FedIPR: Ownership Verification for Federated Deep Neural Network Models

Bowen Li, Lixin Fan, *Member, IEEE*, Hanlin Gu, Jie Li, *Senior Member, IEEE*,
and Qiang Yang, *Fellow, IEEE*

Abstract—Federated learning models are collaboratively developed upon valuable training data owned by multiple parties. During the development and deployment of federated models, they are exposed to risks including illegal copying, re-distribution, misuse and/or free-riding. To address these risks, the ownership verification of federated learning models is a prerequisite that protects federated learning model intellectual property rights (IPR) i.e., FedIPR. We propose a novel federated deep neural network (FedDNN) ownership verification scheme that allows private watermarks to be embedded and verified to claim legitimate IPR of FedDNN models. In the proposed scheme, each client independently verifies the existence of the model watermarks and claims respective ownership of the federated model without disclosing neither private training data nor private watermark information. The effectiveness of embedded watermarks is theoretically justified by the rigorous analysis of conditions under which watermarks can be privately embedded and detected by multiple clients. Moreover, extensive experimental results on computer vision and natural language processing tasks demonstrate that varying bit-length watermarks can be embedded and reliably detected without compromising original model performances. Our watermarking scheme is also resilient to various federated training settings and robust against removal attacks.

Index Terms—Model IPR protection, ownership verification, federated learning, model watermarking, backdoor training.

1 INTRODUCTION

THE successful applications of deep neural network (DNN) to computer vision, natural language processing and data mining tasks come at the cost of the expensive training process: a) the training incurs substantial efforts and costs in terms of expertise, dedicated hardware, and exceedingly long time for the designing and training DNN models; b) it requires a vast amount of training data to boost the model performance, which often increases monotonically with the volume of training data [1], [2], [3], [4]. To protect both the valuable training data and the trained DNN models from being illegally copied, re-distributed or misused, therefore, becomes a compelling need that motivates our research work reported in this article.

To protect the Intellectual Property Rights (IPR) of Deep Neural Network, DNN watermarking techniques have been proposed in [5], [6], [7], [8], [9], [10], [11], [12] to embed designated watermarks into DNN models. Subsequently, DNN ownership is verified by robustly extracting the embedded watermarks from the model in question. Note that both *feature-based watermarks* [9], [10], [11] and *backdoor-based watermarks* [12] have been proposed to verify ownership of DNN models. In order to protect valuable training data in a collaborative learning setting whereas *semi-honest* adversaries may attempt to spy participants' private information, a secure federated learning (SFL) framework has been proposed [13], [14], [15] to collaboratively train a federated deep neural network (FedDNN) without giving away to adversaries private training

data [16] and data feature distribution [17]. Therefore, each client in federated learning must a) *not* disclose to other parties any information about private training data; and b) prove ownership of the trained model without disclosing their private watermarks. The first requirement has been fulfilled by protecting the exchanged local models using techniques such as homomorphic encryption (HE) [18], differential privacy (DP) [19] or secret sharing [20]. The second requirement is one of the open problems considered in this work.

Taking into consideration threat models in both DNN watermarking and secure federated learning, we propose a unified framework called FedIPR which consists of two separate processes along with standard SFL learning procedures: a) *a watermark embedding process* that allows multiple parties to embed their secret feature-based and backdoor-based watermarks; b) *a verification process* that allows each party to independently verify the ownership of FedDNN model.

Two technical challenges for embedding watermarks into FedDNN model are investigated in this paper:

- **Challenge A:** *how to ensure that private watermarks embedded by different clients into the same FedDNN model do not discredit each other?* This challenge is unique in a federated learning setting whereas different client's watermarks may potentially conflict with each other (see Fig. 3 for an example). As a solution to the challenge, theoretical analysis in Theorem 1 elucidates conditions under which multiple feature-based watermarks can be embedded into the same FedDNN model without bringing each other into discredit, and based on the theoretical analysis, a feature-based watermarking method dedicated for horizontal federated learning is proposed. (see Sect. 5.3 for details).
- **Challenge B:** *how to ensure that embedded watermarks*

- Bowen Li and Jie Li are with the Department of Computer Science and Engineering, Shanghai Jiao Tong University, Shanghai 200240, China. The work is done when Bowen Li is an intern at WeBank. E-mail: {li-bowen, lijiecs}@sjtu.edu.cn.
- Lixin Fan and Hanlin Gu are with WeBank AI Lab, WeBank, China. E-mail: lixinfan@webank.com, {Lixin.Fan01, ghltsl123}@gmail.com.
- Qiang Yang is with the Department of Computer Science and Engineering, Hong Kong University of Science and Technology, Hong Kong and WeBank AI Lab, WeBank, China. E-mail: qyang@cse.ust.hk.

are robust to privacy-preserving learning strategies? This challenge is due to modifications of model parameters brought by various privacy preserving methods e.g., differential privacy [19], defensive aggregation [21], [22], [23] and client selection [13]. As a solution, FedIPR adopts robust client-side training to embed both feature-based and backdoor-based watermarks. Our empirical results in Sect. 6 show that robust feature-based and backdoor-based watermarks are persistent under various federated learning strategies.

Moreover, extensive experiments on computer vision and natural language processing tasks demonstrate that feature-based watermarks embedded in *normalization scale parameters* (see Sect. 5.3 for details) are highly reliable, while backdoor-based watermarks can be reliably detected for black-box ownership verification. In short, main contributions of our work are threefold:

- We put forth the first general framework called FedIPR for ownership verification of DNN models in a secure federated learning setting. FedIPR is designed in such a way that each client can embed his/her own private feature-based and backdoor-based watermarks and verify watermarks to claim ownership independently.
- We demonstrate successful applications of FedIPR for various DNN model architectures trained in the semi-honest federated learning setting. Theoretical analysis of the *significance* of feature-based watermarks and superior performance with extensive experimental results showcase the efficacy of the proposed FedIPR framework.
- FedIPR also provides an effective method to detect freeriders [24], [25] who do not contribute data or computing resources but participate in federated learning to get for free the valuable model. Due to the lack of rightful watermarks embedded in the FedDNN model, freeriders can be discerned from benign participants.

To our best knowledge, the FedIPR framework is the first technical solution that supports the protection of DNN ownerships in a secure federated learning setting such that secret watermarks embedded in FedDNN models do not disclose to semi-honest adversaries.

The rest of the paper is organized as follows: Section 2 briefly reviews previous work related to secure federated learning and DNN ownership verification. Section 3 describes the preliminary background for FedIPR. Section 4 illustrates the proposed FedIPR framework formulation. Section 5 delineates the watermark embedding approaches both in white-box and black-box modes, and Section 6 presents experimental results and showcases the robustness of FedIPR. We discuss and conclude the paper in Section 7.

2 RELATED WORK

We briefly review related work in three following aspects and refer readers to survey articles in respective aspects [15], [26], [27].

2.1 Secure Federated Learning

Secure Federated learning [13], [14], [15] aims to collaboratively train a global machine learning model among multiple clients without disclosing private training data to each other [18], [19], [20], [28]. Moreover, privacy-preserving techniques such as homomorphic encryption [18], differential privacy [19] and secret

sharing [20] were often used to protect exchanged local models [13], [14].

2.2 Threats to Model IPR

It was shown that FedDNN models of high commercial values were subjected to severe IPR threats [24], [29], [30], [31]. Firstly, unauthorized parties might plagiarize the DNN model with non-technical methods [29]. Secondly, Tramer et al. showcased *model stealing attacks* that aimed to steal deployed victim models even if attackers have no knowledge of training samples or model parameters [30]. Thirdly, Fraboni et al. demonstrated that *freeriders* might join in federated learning and plagiarized the valuable models with no real contributions to the improvements of federated models [24].

2.3 DNN Watermarking Methods

As a counter measure against model plagiarisms, two categories of DNN watermarking methods have been proposed.

Backdoor-based methods proposed to use a particular set of inputs as the triggers and let the model deliberately output specific incorrect labels [12], [32], [33]. Backdoor-based methods collected evidence of suspected plagiarism through remote API without accessing internal parameters of models.

Feature-based methods proposed to encode designated binary strings as watermarks into layer parameters in DNN models [5], [9], [10], [11], [34]. Specifically, Uchida et al. [9] proposed to embed feature-based watermarks into convolution layer weights using a binary cross-entropy loss function. Fan et al. [35] proposed to embed feature-based watermarks into *normalization layer scale parameters* of the convolution block with a hinge-like regularization term. In the verification stage of feature-based watermarks, one must access DNN internal parameters to detect watermarks. We also refer to a recent survey [27] for more existing watermark embedding schemes.

Also for federated learning model ownership verification, Atli et al. [36] adopted *backdoor-based* watermarks to enable ownership verification for the central server. Nevertheless, they only considered the setting in which the server was responsible for embedding watermarks into the global FedDNN model, and did not allow clients to embed and verify private watermarks.

3 PRELIMINARIES

In this section, we first review and formulate key ingredients of the secure horizontal federated learning and existing DNN watermarking methods as follows. We also explain in Tab. 1 all notations used in this article.

3.1 Secure Horizontal Federated Learning

A secure horizontal federated learning [14] system consists of K clients which build local models¹ with their own data and send local models $\{\mathbf{W}_k\}_{k=1}^K$ to an aggregator to obtain a global model. The aggregator conducts the following aggregation process [13], [14], [15]:

$$\mathbf{W} \leftarrow \sum_{k=1}^K \frac{n_k}{K} \mathbf{W}_k, \quad (1)$$

1. Other works [13] also call them model updates, because the local models are equal to model updates for aggregation.

where n_k is the weight for each client's local model \mathbf{W}_k .

Remark: in secure federated learning, local model \mathbf{W}_k might be protected by using Homomorphic Encryption (HE) [18], Differential Privacy (DP) [19] such that semi-honest adversaries can not infer private information from \mathbf{W}_k . These privacy preserving strategies pose one challenge to be addressed for reliable watermarking (see Sect. 4.3).

3.2 Freeriders in Federated Learning

In federated learning, there might be *freerider* clients [24] who do not contribute data or computing resources but construct some superficial local models to participate in training only to obtain the global model for free. Specifically, there are several strategies for freeriders to construct local models [24]:

Freeriding with Previous Models (Plain Freerider). Freeriders create a superficial model as follows [24],

$$\mathbf{W}^{free} = Free(\mathbf{W}^t, \mathbf{W}^{t-1}), \quad (2)$$

in which $\mathbf{W}^t, \mathbf{W}^{t-1}$ denote respectively local models from two previous iterations. Note that the construction of this superficial model costs nothing for freeriders since they are merely saved copies of model parameters from previous iterations.

Freeriding with Gaussian Noise. Freeriders adopt the previous global model parameters \mathbf{W}^{t-1} and add Gaussian noise to simulate a local model:

$$\mathbf{W}^{free} = \mathbf{W}^t + \xi_t, \quad \xi_t \sim \mathcal{N}(0, \sigma_t). \quad (3)$$

Detection methods are proposed to detect and eliminate superficial local models as such [25]. However it is required to train a meta freerider detector.

Notations	Descriptions
K	Number of clients in Secure Federated Learning
\mathbb{N}	Federated neural network model
\mathbf{W}	Model weights of model \mathbb{N}
\mathbf{W}_k	Local model of k -th client \mathbb{N}
$\mathcal{G}()$	Key Generation Process
$N_{\mathbf{T}}$	Bit-length of backdoor-based watermarks
\mathbf{T}	Target <i>backdoor-based</i> watermarks
$(\mathbf{X}_{\mathbf{T}}, \mathbf{Y}_{\mathbf{T}})$	Samples and labels of backdoor-based watermarks \mathbf{T}
N	Bit-length of feature-based watermarks
\mathbf{B}	Target <i>feature-based</i> watermarks
$\tilde{\mathbf{B}}$	<i>Feature-based</i> watermarks extracted from the parameters
$\theta = \{\mathbf{S}, \mathbf{E}\}$	Secret parameters for <i>feature-based</i> watermarks
\mathbf{S}	Watermark location parameters
\mathbf{E}	Watermark embedding matrix
$\mathcal{E}()$	Watermark Embedding Process
\mathbf{W}_k^t	Local model of k -th client at communication round t
\mathbf{W}^t	Global model at communication round t
L_D	The loss function for the main learning task
$L_{\mathbf{T}}$	Backdoor-based watermark embedding regularization term
$L_{\mathbf{B}, \theta}$	Feature-based watermark embedding regularization term
$\mathcal{A}()$	Aggregation Process in Secure Federated Learning
$\mathcal{V}()$	Watermark Verification Process
$\mathcal{V}_W()$	White-box verification
$\mathcal{V}_B()$	Black-box verification
η_F	Detection rate of feature-based watermarks
η_T	Detection rate of backdoor-based watermarks

TABLE 1: Notations used in this article.

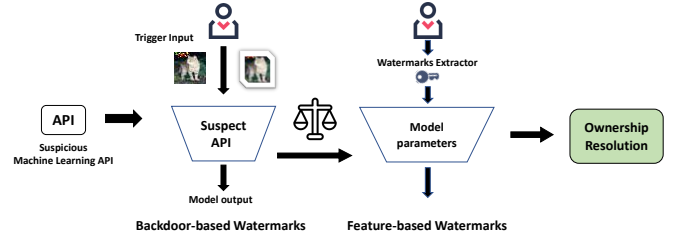


Fig. 1: Ownership verification processes composed of backdoor-based watermarks and feature-based watermarks

3.3 DNN Watermarking Methods

There are broadly two categories of DNN watermarking methods: **Feature-based Watermarks** [9], [10], [11], [35]. In the watermark embedding step, N -bits target binary watermarks $\mathbf{B} \in \{0, 1\}^N$ are embedded during the learning of model parameters \mathbf{W} , by adding regularization terms to the original learning task.

During the verification step, feature-based watermarks $\tilde{\mathbf{B}}$ extracted with extractor θ from DNN parameters is then matched with the designated watermarks \mathbf{B} , to judge if Hamming distance $H(\mathbf{B}, \tilde{\mathbf{B}})$ is less than a preset threshold ϵ_W :

$$\mathcal{V}_W(\mathbf{W}, (\mathbf{B}, \theta)) = \begin{cases} \text{TRUE}, & \text{if } H(\mathbf{B}, \tilde{\mathbf{B}}) \leq \epsilon_W, \\ \text{FALSE}, & \text{otherwise,} \end{cases} \quad (4)$$

in which $\mathcal{V}_W()$ is the ownership verification process that has to access model parameters in a white-box mode.

Backdoor-based Watermarks [12], [33]. Backdoor-based watermarks $\mathbf{T} = \{(\mathbf{X}_{\mathbf{T}}^1, \mathbf{Y}_{\mathbf{T}}^1), \dots, (\mathbf{X}_{\mathbf{T}}^{N_{\mathbf{T}}}, \mathbf{Y}_{\mathbf{T}}^{N_{\mathbf{T}}})\}$ are embedded into the model function \mathbb{N} during the training time by incorporating a loss function of backdoor samples.

In the verification step, backdoor samples are used as the trigger input to the model \mathbb{N} . The ownership is successfully verified if the detection error of designated backdoor labels is less than a threshold ϵ_B :

$$\mathcal{V}_B(\mathbb{N}, \mathbf{T}) = \begin{cases} \text{TRUE}, & \text{if } \mathbb{E}_{\mathbf{T}_n}(\mathbb{I}(\mathbf{Y}_{\mathbf{T}} \neq \mathbb{N}(\mathbf{X}_{\mathbf{T}}))) \leq \epsilon_B, \\ \text{FALSE}, & \text{otherwise,} \end{cases} \quad (5)$$

in which $\mathcal{V}_B()$ is the ownership verification process that only accesses model API in black-box mode.

Remark: $(\mathbf{B}, \theta, \mathbf{T})$ are private watermarking information that should be kept secret without disclosing to other parties.

4 FEDERATED DNN OWNERSHIP VERIFICATION

We propose a novel watermark embedding and ownership verification scheme called FedIPR for the secure horizontal federated learning scenario. FedIPR is designed in the way such that each client can a) protect his/her private data; and b) embed and verify his/her own private watermarks without disclosing information about private watermarks.

4.1 FedIPR: FedDNN Ownership Verification with Watermarks

Following the framework of SFL in Sect. 3.1, we give below a formal definition of the FedIPR ownership verification scheme, which is pictorially illustrated in Fig. 2.

Definition 1. A Federated Deep Neural Network (FedDNN) model ownership verification scheme (FedIPR) for a given network $\mathbb{N}[\]$ is

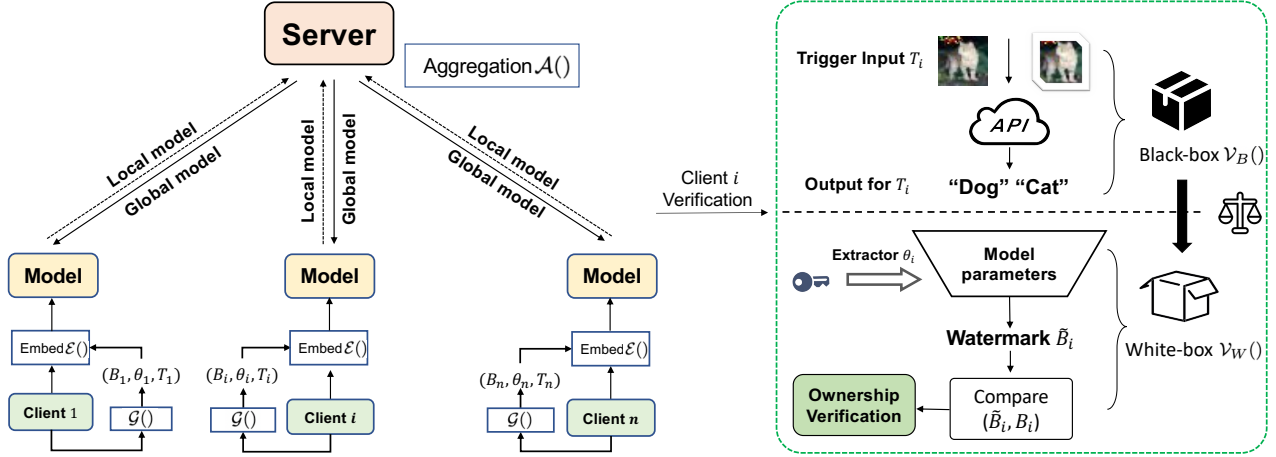


Fig. 2: An illustration of federated DNN (FedDNN) watermark Embedding and Verification scheme. Private watermarks are generated and embedded into the local models, which are then aggregated using the FedAvg algo. (the left panel). In case the federated model is plagiarized, each client may invoke verification processes to extract watermarks from the plagiarized model in both black-box and white-box manner to claim his/her ownership of the federated model (the right panel).

defined as a tuple $\mathcal{V} = (\mathcal{G}, \mathcal{E}, \mathcal{A}, \mathcal{V}_W, \mathcal{V}_B)$ of processes, consisting of:

- I) For client $k \in \{1, \dots, K\}$, a client-side *key generation process* $\mathcal{G}() \rightarrow (\mathbf{B}_k, \theta_k, \mathbf{T}_k)$ generates target watermarks \mathbf{B}_k , watermark extraction parameters $\theta_k = \{\mathbf{S}_k, \mathbf{E}_k\}$ and a *trigger set* (backdoor-based watermarks) $\mathbf{T}_k = \{(\mathbf{X}_{\mathbf{T}_k}^1, \mathbf{Y}_{\mathbf{T}_k}^1), \dots, (\mathbf{X}_{\mathbf{T}_k}^{N_{\mathbf{T}}}, \mathbf{Y}_{\mathbf{T}_k}^{N_{\mathbf{T}}})\}$; **Remark:** the $(\mathbf{B}_k, \theta_k, \mathbf{T}_k)$ are private watermarking parameters that should be kept secret without disclosing to other clients. In the extraction parameters $\theta_k = \{\mathbf{S}_k, \mathbf{E}_k\}$, \mathbf{S}_k denotes the location of watermarks \mathbf{B}_k , and \mathbf{E}_k denotes the secret extraction matrix for watermarks \mathbf{B}_k .
- II) A client-side FedDNN *embedding process* $\mathcal{E}()$ minimizes the combined loss L_k of the main task, and two regularization terms $L_{\mathbf{T}_k}$ and $L_{\mathbf{B}_k, \theta_k}$ to embed trigger samples \mathbf{T}_k and feature-based watermarks \mathbf{B}_k respectively², once receives the global model \mathbf{W}^t at communication round t ,

$$L_k := \underbrace{L_{D_k}(\mathbf{W}^t)}_{\text{main task}} + \alpha_k \underbrace{L_{\mathbf{T}_k}(\mathbf{W}^t)}_{\text{backdoor-based}} + \beta_k \underbrace{L_{\mathbf{B}_k, \theta_k}(\mathbf{W}^t)}_{\text{feature-based}}, \quad k \in \{1, \dots, K\}, \quad (6)$$

where D_k denotes the training data of client k , α_k ³ denotes the parameters to control the backdoor-based watermarking loss $L_{\mathbf{T}_k}$, and β_k denotes the factor for feature-based watermarking regularization term $L_{\mathbf{B}_k, \theta_k}$.

Remark: Note that a $\text{ClientUpdate}(L_k, \mathbf{W}^t) =: \text{argmin} L_k$ sub-routine seeks the optimal parameters and sends local model to the aggregator (see below for a server-side aggregation process).

- III) A server-side FedDNN *aggregation process* $\mathcal{A}()$ collects local models from m randomly selected clients and performs model aggregation using the FedAvg algorithm [13] i.e.,

$$\mathbf{W}^{t+1} \leftarrow \sum_{k=1}^K \frac{n_k}{n} \mathbf{W}_k^{t+1}, \quad (7)$$

2. A client k may opt-out and not embed watermarks or trigger samples by setting $\alpha_k = 0.0$ or $\beta_k = 0.0$. Following [37], we adopt a *random sampling* strategy in experiments to assign non-zero values to α_k, β_k to simulate the situation that clients make decisions on their own.

3. If backdoor samples are filled in batches in the implementation side of backdoor-based watermarking task, the parameter α_k is equal to 1

where $\mathbf{W}_k^{t+1} \leftarrow \text{ClientUpdate}(L_k, \mathbf{W}^t)$ is the local model of client k at round t , and $\frac{n_k}{n}$ denoted the aggregation weight for Fedavg algorithm.

Remark: in SFL, strategies like Differential Privacy [38], defensive aggregation mechanism [21], [22], [23] and client selection [13] are widely used for privacy, security and efficiency.

After the global model \mathbf{W} is trained with convergence, each client can conduct ownership verification as follows.

- IV) A client-side *black-box verification process* $\mathcal{V}_B()$ checks whether the detection error of designated labels $\mathbf{Y}_{\mathbf{T}_k}$ generated by trigger samples $\mathbf{X}_{\mathbf{T}_k}$ is smaller than ϵ_B ,

$$\mathcal{V}_B(\mathbf{N}, \mathbf{T}_k) = \begin{cases} \text{TRUE}, & \text{if } \mathbb{E}_{\mathbf{T}_k}(\mathbb{I}(\mathbf{Y}_{\mathbf{T}_k} \neq \mathbf{N}(\mathbf{X}_{\mathbf{T}_k}))) \leq \epsilon_B, \\ \text{FALSE}, & \text{otherwise,} \end{cases} \quad (8)$$

in which $\mathbb{I}()$ is the indicator function and \mathbb{E} the expectation over trigger set \mathbf{T}_k .

- V) A client-side *white-box verification process* $\mathcal{V}_W()$ extracts feature-based watermarks $\tilde{\mathbf{B}}_k = \text{sgn}(\mathbf{W}, \theta_k)$ with sign function $\text{sgn}()$ from the global model parameters \mathbf{W} , and verifies the ownership as follows,

$$\mathcal{V}_W(\mathbf{W}, (\mathbf{B}_k, \theta_k)) = \begin{cases} \text{TRUE}, & \text{if } H(\mathbf{B}_k, \tilde{\mathbf{B}}_k) \leq \epsilon_W, \\ \text{FALSE}, & \text{otherwise,} \end{cases} \quad (9)$$

in which $H(\mathbf{B}_k, \tilde{\mathbf{B}}_k)$ is the Hamming distance between $\tilde{\mathbf{B}}_k$ and the target watermarks \mathbf{B}_k , and ϵ_W is a preset threshold.

Watermark Detection Rate. For client ownership verification, the *watermark detection rate* can be defined as:

- For N bit-length feature-based watermarks \mathbf{B} , detection rate η_F is calculated as

$$\eta_F := 1 - \frac{1}{N} H(\mathbf{B}, \tilde{\mathbf{B}}), \quad (10)$$

where $H(\mathbf{B}, \tilde{\mathbf{B}})$ measures Hamming distance between extracted binary watermark string $\tilde{\mathbf{B}}$ and the target watermarks \mathbf{B} ;

- For backdoor-based watermarks \mathbf{T} , the detection rate is

$$\eta_T := \mathbb{E}_{\mathbf{T}}(\mathbb{I}(\mathbf{Y}_{\mathbf{T}} = \mathbf{N}(\mathbf{X}_{\mathbf{T}}))), \quad (11)$$

which is calculated as the ratio of backdoor samples that are classified as designated labels w.r.t. the total number N_T of trigger set.

Given the definition of FedIPR, let us proceed to illustrate two technical challenges to be addressed by FedIPR.

4.2 Challenge A: Conflicting goals of more than one watermarks in FedDNN

For all clients, the *watermark capacity* measures the overall bit-length of watermarks that can be significantly verified. The first challenge is to determine the maximal capability of multiple watermarks that can be embedded by K clients in SFL without discrediting each other.

Specifically for *feature-based* watermarks, it remains an open question whether there is a common solution for different clients to embed their private designated watermarks. To illustrate the potential conflict between watermarks assigned by different clients, let us investigate the following examples:

Example 1: two clients need to embed different watermarks $\mathbf{B}_1 = 010$ and $\mathbf{B}_2 = 101$, respectively, into the same parameters $\mathbf{W} = (w_1, w_2, w_3, w_4, w_5)$ with the same embedding matrix

$$\mathbf{E} = \begin{pmatrix} e_{11} & e_{12} & e_{13} & e_{14} & e_{15} \\ e_{21} & e_{22} & e_{23} & e_{24} & e_{25} \\ e_{31} & e_{32} & e_{33} & e_{34} & e_{35} \end{pmatrix}^T, \quad (12)$$

the watermarks extracted from parameters $\mathbf{W} = (w_1, w_2, w_3, w_4, w_5)$ are $\tilde{\mathbf{B}} = \mathbf{WE}$, and they add regularization terms constraining the parameters to satisfy:

$$\begin{cases} (010): & \sum_{i=1}^5 w_i e_{1i} < 0, \sum_{i=1}^5 w_i e_{2i} > 0, \sum_{i=1}^5 w_i e_{3i} < 0, \\ (101): & \sum_{i=1}^5 w_i e_{1i} > 0, \sum_{i=1}^5 w_i e_{2i} < 0, \sum_{i=1}^5 w_i e_{3i} > 0, \end{cases} \quad (13)$$

it is obvious that two different watermarks again impose conflicting constraints that cannot be simultaneously satisfied by the same global model parameters.

General Case: for the feature-based watermarks $\{(\mathbf{B}_k, \theta_k)\}_{k=1}^K$ embedded into the same model parameters \mathbf{W} by K different clients, each client k embeds N bit-length of feature-based watermarks $\mathbf{B}_k = (t_{k1}, t_{k2}, \dots, t_{kN}) \in \{+1, -1\}^N$, the extracted watermarks $\tilde{\mathbf{B}}_k = \mathbf{WE}_k$ should be consistent with targeted watermarks \mathbf{B}_k :

$$\forall j \in \{1, 2, \dots, N\} \quad \text{and} \quad k \in K, t_{kj}(\mathbf{WE}_k)_j > 0. \quad (14)$$

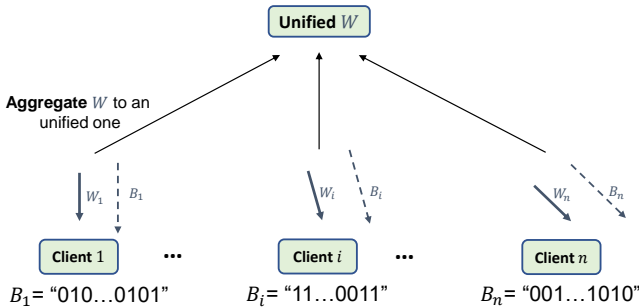


Fig. 3: Different clients in federated learning adopt different regularization terms to embed feature-based watermarks

As Fig. 3 shows, each client k tries to guide the target parameter \mathbf{W}_k to a special direction conditioned on \mathbf{B}_k , but each \mathbf{W}_k is

aggregated into an unified \mathbf{W} according to Eq. (7) in SFL, these constraints may conflict with each other.

Theorem 1 elucidates the condition under which a feasible solution exists for K different watermarks to be embedded without conflicts and provides the lower bound of detection rate η_F .

Theorem 1. For K different watermarks (N bit-length each) to embed in M channels of the global model parameters \mathbf{W} , take their detection rate to be measured as $\eta_F = 1 - \frac{1}{N}H(\mathbf{B}, \tilde{\mathbf{B}})$, where $H(\mathbf{B}, \tilde{\mathbf{B}})$ is the hamming distance between extracted watermarks $\tilde{\mathbf{B}}$ and the target watermarks \mathbf{B} . The watermark detection rate η_F satisfies:

Case 1: If $KN \leq M^4$, then there exists \mathbf{W} such that

$$\eta_F = 1. \quad (15)$$

Case 2: If $KN > M$, then, there exists \mathbf{W} such that

$$\eta_F \geq \frac{KN + M}{2KN}. \quad (16)$$

The proof is deferred in Appendix A.

Remark: results in **case 1** ($KN < M$) demonstrate the existence of a solution for watermark embedding when the total bit-length of all clients' watermarks KN is smaller than the total number M^5 of network channels that can be used to embed watermarks; results in **case 2** ($KN > M$) provides a lower bound of detection rate of embedded watermarks. For example, if $K = 10$ clients decide to each embed $N = 100$ bit-length watermarks into $M = 600$ channels of model parameters \mathbf{W} , the lower bound of detection rate is $\eta_F = 0.8$.

Taking both cases into account, we give below the optimal bit-length assigned to multiple watermarks under different situations (detailed analysis is deferred to Appendix B).

Optimal bit-length and maximal bit-length N^6 . We treat feature-based ownership verification as a hypothesis testing, where \mathcal{H}_0 is "the model is not plagiarized" versus \mathcal{H}_1 "model is plagiarized", and we get p-value as the statistical significance of watermarks, the upper bound is given:

$$p\text{-value} \leq \sum_{i=\eta_F N}^N \binom{N}{i} (1/C)^i (1 - 1/C)^{N-i}, \quad (17)$$

in which $C = 2$.

With analysis of p-value (see detailed analysis in Appendix B), the optimal bit-length for the smallest p-value is

$$N_{opt} = M/K. \quad (18)$$

The optimal bit-length is determined by the "smallest p-value" i.e., the most significant watermark verification.

In case that a p-value is only required to be less than a given statistical significance level α e.g., 0.0001, we can determine the

4. Another condition for this theorem is the embedding matrix \mathbf{E} clients decide needs to be column (line) non-singular matrix (see the detail in Appendix A)

5. For example, $M = 896$ channels across the last 3 layers for AlexNet, $M = 2048$ channels across the last 4 layers for ResNet18 and $M = 2304$ channels across the last 3 layers for DistilBERT (illustrated in Appendix C).

6. However, other factors may influence η_F . For example, as experiment results in Fig. 12, 10 demonstrated, random noise added to the federated learning process or removal attacks launched by plagiarizers, all conspire to degrade η_F to various extents.

range of bit-length N (N_{max} and N_{min}) that can guarantee that p-value is lower than the given level α . Take an example as in Fig. 1, if $K = 10$ clients decide to embed watermarks into $M = 896$ channels of model parameters, $N_{opt} = 90$, when $\alpha = 0.0001$, the corresponding N_{max} is 550 and N_{min} is 18.

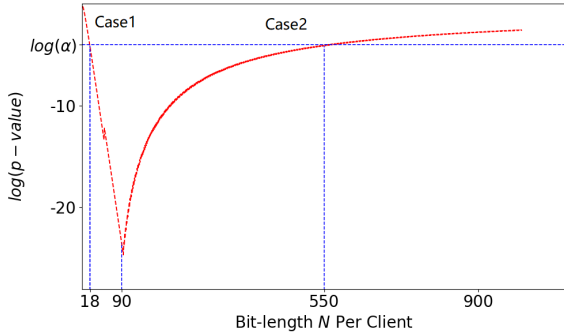


Fig. 4: The optimal bit-length and the acceptable range of watermark bit-length that provide strong confidence of ownership verification. As shown in figure, $K = 10$, $M = 896$, and $\eta_F = 0.98$ (we take by default) in case 1, the optimal bit-length for p-value is $N_{opt} = M/K = 90$, for an acceptable level $\alpha = 0.0001$, the acceptable range of watermark bit-length is from $N = 18$ to $N = 550$.

In short, analysis of Theorem 1 specifies the optimal bit-length and the acceptable range of watermark bit-length that allows reliable detection rates with sufficient significance to support ownership verification. Moreover, it is shown that empirical results in Sect. 6 are in accordance with the analysis elucidated in this section.

4.3 Challenge B: Robustness of Watermarks in FedDNN

The robustness of watermarks indicates whether the detection rate is persistent against various training strategies and attacks that attempt to remove the watermarks.

We investigate the robustness of both the feature-based and backdoor-based watermarks in the FedDNN model. Particularly, we measure the detection rate and statistical significance of watermarks with/without training strategies and attacks to report the robustness. The measurement settings including impacting factors (training strategies and attacks), targeted watermarks (feature-based watermarks in Normalization parameters \mathbf{W}_γ and convolution parameters \mathbf{W}_C and backdoor-based watermarks), and metrics are summarized in Tab. 2:

Impacting factor	Watermarks		Metrics	
	feature-based	backdoor-based	Detection Rate	p-value
Differential Privacy	\mathbf{W}_γ	✓	✓	✓
Client Selection	\mathbf{W}_γ	✓	✓	✓
Defensive Aggregation	\mathbf{W}_γ	✓	✓	✓
Pruning Attack	$\mathbf{W}_\gamma, \mathbf{W}_C$	✓	✓	
Fine-tuning Attack	$\mathbf{W}_\gamma, \mathbf{W}_C$	✓	✓	

TABLE 2: Reported investigation setting of robustness.

Training Strategies: In SFL, strategies like differential privacy [38], defensive aggregation mechanism [21], [22], [23] and client selection [13] are widely used for privacy, security and efficiency. Those training strategies modify the training processes of SFL,

which may affect the detection rate i.e., the significance of watermarks:

- To protect data privacy, *differential privacy* mechanism [19] in SFL add noise to the local model of each client.
- For defending the model poisoning attack [21], [39], *defensive aggregation* [21], [22], [23] in SFL perform detect and filter some local models from each client.
- For communication efficiency, in each communication round, the server adopts certain *client selection* strategies [13] to pick up a random subset of clients and have their local models aggregated. Other clients do not need to upload local models until they are selected in future communication rounds.

Removal Attack. The attacker that steals the model may try to remove the watermarks while inheriting most model performance. Following previous DNN watermarking methods [5], [7], [12], we investigate watermark robustness under *fine-tuning* and *pruning* attacks (see Algo. 1 for pseudocodes).

Algorithm 1: Removal attack

Input: Model \mathbb{N} , pruning rate p , additional training data D_{add} .

- 1: **procedure** PRUNING
- 2: Pruning the model \mathbb{N} with p pruning rate.
- 3: **procedure** FINETUNING
- 4: **for** epochs in 50 **do**
- 5: Train the model \mathbb{N} only in main classification task with additional training data D_{add} .

We adopt client-side watermark embedding method to investigate the watermark robustness. Extensive experimental results in Sect. 6.5 show that both backdoor-based and feature-based watermarks can be reliably detected with high significance (p-value less than $2.89e^{-15}$ is guaranteed).

5 IMPLEMENTATION OF FEDDNN OWNERSHIP VERIFICATION

Sect. 4 proposes the FedIPR framework, which allows clients to independently embed secret watermarks into the model and verify whether the designated watermarks exist in the model in question. We illustrate below a specific implementation of FedIPR framework with algorithm pseudocodes given in Algo. 2, 3 and 4.

5.1 Watermark Generation

For a client k in the federated learning system, the watermarks adopted to mark trained FedDNN model include backdoor-based watermarks \mathbf{T}_k and feature-based watermarks (\mathbf{B}_k, θ_k) . Those watermarks are initialized and kept in secret as shown in Algo. 2.

Algorithm 2: Generation $\mathcal{G}()$ of Watermarks

- 1: **procedure** WATERMARK GENERATION
- 2: **for** client k in K clients **do**
- 3: Initialize $(\mathbf{B}_k, \theta_k) = \{\mathbf{S}_k, \mathbf{E}_k\}$.
- 4: Encode \mathbf{B}_k into binary string.
- 5: Initialize $\mathbf{T}_k = \{(\mathbf{X}_{\mathbf{T}_k}^1, \mathbf{Y}_{\mathbf{T}_k}^1), \dots, (\mathbf{X}_{\mathbf{T}_k}^{N_{\mathbf{T}}}, \mathbf{Y}_{\mathbf{T}_k}^{N_{\mathbf{T}}})\}$.
▷ Trigger samples $\mathbf{X}_{\mathbf{T}_k}$ and corresponding output labels $\mathbf{Y}_{\mathbf{T}_k}$.
- 6: **return** $\{(\mathbf{B}_k, \theta_k, \mathbf{T}_k)\}_{k=1}^{K=K}$

As illustrated in Algo. 3, the client-side FedDNN *embedding process* $\mathcal{E}()$ minimizes the weighted combined loss of main task and two regularization terms to embed watermarks \mathbf{T}_k and \mathbf{B}_k respectively.

5.2 Backdoor-based Watermark Embedding and Verification

To embed backdoor-based watermarks $\mathbf{T}_k = \{(\mathbf{X}_{\mathbf{T}_k}^1, \mathbf{Y}_{\mathbf{T}_k}^1), \dots, (\mathbf{X}_{\mathbf{T}_k}^{N_{\mathbf{T}}}, \mathbf{Y}_{\mathbf{T}_k}^{N_{\mathbf{T}}})\}$, the model owner train the model with an additional backdoor training task where the loss function of backdoor training $L_{\mathbf{T}}(\mathbf{W}^t)$ is defined with cross entropy (CE) loss:

$$L_{\mathbf{T}}(\mathbf{W}^t) = CE(\mathbf{Y}_{\mathbf{T}_k}, \mathbb{N}(\mathbf{X}_{\mathbf{T}_k})). \quad (19)$$

Adversarial Samples as Triggers. In our FedIPR scheme, we adopt adversarial samples as the triggers. Basically, adversarial samples $(\mathbf{X}_{\mathbf{T}}, \mathbf{Y}_{\mathbf{T}})$ are generated from original data (\mathbf{X}, \mathbf{Y}) with Projected Gradient Descent (PGD) [40]. Our backdoor-based watermark scheme adopts those backdoor samples as the trigger input during both training time and inference time.

Each backdoor-based watermarks $\mathbf{X}_{\mathbf{T}}$ is verified, provided that for the input $\mathbf{X}_{\mathbf{T}}$, the model outputs the designated label,

$$\mathbb{N}(\mathbf{X}_{\mathbf{T}}) = \mathbf{Y}_{\mathbf{T}}. \quad (20)$$

5.3 Feature-based Watermark Embedding and Verification

In FedIPR, each client k chooses its own (\mathbf{B}_k, θ_k) as the feature-based watermarks, which are embedded with a regularization term $L_{\mathbf{B}_k, \theta_k}$ along with main task loss.

Approach of FedIPR. FedIPR proposes that each client embeds its own watermarks \mathbf{B}_k with secret parameters $\theta_k = (\mathbf{S}_k, \mathbf{E}_k)$:

$$L_{\mathbf{B}_k, \theta_k}(\mathbf{W}^t) = L_{\mathbf{B}_k}(\mathbf{S}_k, \mathbf{W}^t, \mathbf{E}_k), \quad (21)$$

whereas the secret watermarking parameters $\theta_k = (\mathbf{S}_k, \mathbf{E}_k)$ are only known for client k , and FedIPR proposes to embed the watermarks into the *normalization layer scale parameters* of the convolution block, i.e., $\mathbf{S}_k(\mathbf{W}) = \mathbf{W}_{\gamma} = \{\gamma_1, \dots, \gamma_C\}$, where C is the number of normalization channels in \mathbf{W}_{γ} .

We adopt a secret embedding matrix $\mathbf{E}_k \in \theta_k = (\mathbf{S}_k, \mathbf{E}_k)$ to embed and extract watermarks, the distance between targeted watermarks and extracted watermarks is implemented as following regularization term:

$$\begin{aligned} L_{\mathbf{B}_k, \theta_k}(\mathbf{W}^t) &= L_{\mathbf{B}_k}(\mathbf{W}_{\gamma}^t \mathbf{E}_k, \mathbf{B}_k) \\ &= \text{HL}(\mathbf{B}_k, \tilde{\mathbf{B}}_k) = \sum_{j=1}^N \max(\mu - b_j t_j, 0), \end{aligned} \quad (22)$$

where we note $\tilde{\mathbf{B}}_k = \mathbf{W}_{\gamma}^t \mathbf{E}_k$ as extracted watermarks and we implement the regularization term as *hinge-like loss* $\text{HL}()$ on the target watermarks $\mathbf{B}_k = (t_1, \dots, t_N) \in \{0, 1\}^N$ and extracted watermarks $\tilde{\mathbf{B}}_k = (b_1, \dots, b_N) \in \{0, 1\}^N$, and μ is the parameter of hinge loss.

In SFL, we implement feature-based watermark embedding for two different network architectures including convolution neural network (CNN) and transformer-based neural network.

Algorithm 3: Embedding Process $\mathcal{E}()$ of Watermarks

- 1: Each client k with its own watermark tuple $(\mathbf{B}_k, \theta_k, \mathbf{T}_k)$
- 2: **for** communication round t **do**
- 3: The server distributes the global model parameters \mathbf{W}^t to each clients and randomly selects cK out of K clients.
- 4: **Local Training:**
- 5: **for** k in selected cK of K clients **do**
- 6: Sample mini-batch of m training samples $\mathbf{X}\{\mathbf{X}^{(1)}, \dots, \mathbf{X}^{(m)}\}$ and targets $\mathbf{Y}\{\mathbf{Y}^{(1)}, \dots, \mathbf{Y}^{(m)}\}$.
- 7: **if** Enable backdoor-based watermarks **then**
- 8: Sample t samples $\{\mathbf{X}_{\mathbf{T}_k}^{(1)}, \dots, \mathbf{X}_{\mathbf{T}_k}^{(t)}\}, \{\mathbf{Y}_{\mathbf{T}_k}^{(1)}, \dots, \mathbf{Y}_{\mathbf{T}_k}^{(t)}\}$ from trigger set $(\mathbf{X}_{\mathbf{T}_k}, \mathbf{Y}_{\mathbf{T}_k})$
- 9: Concatenate \mathbf{X} with $\{\mathbf{X}_{\mathbf{T}_k}^{(1)}, \dots, \mathbf{X}_{\mathbf{T}_k}^{(t)}\}$, \mathbf{Y} with $\{\mathbf{Y}_{\mathbf{T}_k}^{(1)}, \dots, \mathbf{Y}_{\mathbf{T}_k}^{(t)}\}$.
- 10: Compute cross-entropy loss L_c using \mathbf{X} and \mathbf{Y} \triangleright
Batch poisoning approach is adopted, thus $\alpha_l = 1$, $L_c = L_{D_{\mathcal{K}}} + L_{\mathbf{T}_k}$.
- 11: **for** layer l in targeted layers set \mathbf{L} **do**
- 12: Compute feature-based regularization term $L_{\mathbf{B}_k, \theta_k}^l$ using θ_k and \mathbf{W}^l
- 13: $L_{\mathbf{B}_k, \theta_k} \leftarrow \sum_{l \in \mathbf{L}} L_{\mathbf{B}_k, \theta_k}^l$
- 14: $L_k = L_c + \beta_k L_{\mathbf{B}_k, \theta_k}$
- 15: Backpropagate using L_k and update \mathbf{W}_k^t
- 16: **Server Update:**
- 17: Aggregate local models $\{\mathbf{W}_k^t\}_{k=1}^K$ with FedAvg algorithm

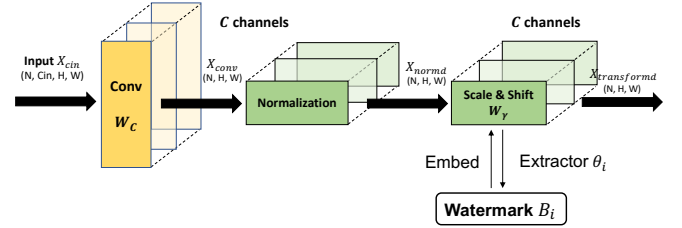


Fig. 5: Layer structure of a convolution layer: normalization layer weights \mathbf{W}_{γ} (in green) are used to embed watermarks, and the watermarks extracted in a white-box manner with a secret extractor matrix.

5.3.1 Feature-based Watermarks in CNN

As illustrated in Fig. 5, for a convolution neural network $\mathbb{N}(\mathbf{W})$, we may choose the convolution kernel weights \mathbf{W}_C or the normalization layer weights \mathbf{W}_{γ} to embed feature-based watermarks.

Fan et al. [35] has reported that normalization layer weights $\mathbf{W}_{\gamma} = (\gamma_1, \dots, \gamma_C) \in \{-1, +1\}^C$ are suitable model parameters to embed robust binary watermark strings as follows:

$$O(x_i^p) = \gamma_i * x_i^p + \beta_i, \quad (23)$$

in which x_i^p is the model parameters in channel i and β_i is the offset parameter of normalization (see [5] and Appendix C for details).

In FedIPR, we choose \mathbf{W}_{γ} to embed feature-based watermarks for robust performance, which is reported in Sect. 6. For ablation study of robustness, we also report watermark performance with other experiment settings in Fig. 12.

5.3.2 Feature-based Watermarks in Transformer-based Networks

As illustrated in Fig. 6, feature-based watermarks can also be applied to transformer-based network. A transformer encoder block [41] is organized with a *Layer-Normalization layer* (the mean output value is normalized in the channel direction, which has an obvious effect for accelerating the convergence performance). The same to normalization in CNN, the process is controlled by parameters \mathbf{W}_γ in the *Layer-Normalization layer*.

In FedIPR, we choose \mathbf{W}_γ to embed the feature-based watermarks, such that the watermarks can be persistent in the model architecture.

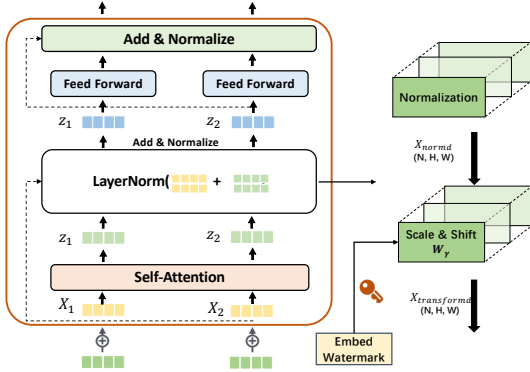


Fig. 6: Layer structure of an encoder block: normalization layer weights \mathbf{W}_γ (in green) are used to embed feature-based watermarks which are extracted in white-box manner.

5.4 Ownership Verification with Watermarks

Once the model is plagiarized by unauthorized party, the model owner can call experiments of ownership verification. As Algo. 4 illustrates, for the backdoor-based watermark verification, the model owner query the API with designed triggers, and for feature-based verification, it detected the feature-based watermarks embedded in the normalization layer according to the sign of according channel parameters. Combined with both backdoor-based and feature-based watermarks, the statistical significance of ownership verification is obtained.

Algorithm 4: Ownership Verification $\mathcal{V}_B()$ and $\mathcal{V}_W()$

Input: API $\mathbb{N}()$ offered by adversaries, Triggers $(\mathbf{X}_T, \mathbf{Y}_T)$ provided by owner; Model weights \mathbf{W} of model, secret parameters $\theta = (\mathbf{S}, \mathbf{E})$ and target watermarks \mathbf{B} provided by user.

- 1: **procedure** WATERMARK DETECTION
- 2: Input the backdoor \mathbf{X}_T into model \mathbb{N} to derive the classification label $\mathbb{N}(\mathbf{X}_T)$
- 3: Match $\mathbb{N}(\mathbf{X}_T)$ with target backdoor label \mathbf{Y}_T
- 4: Compute the backdoor detection rate $\eta_T = \mathcal{V}_B(\mathbf{X}_T, \mathbf{Y}_T, \mathbb{N})$
- 5: $\tilde{\mathbf{B}} \leftarrow \text{sgn}(\mathbf{S}(\mathbf{W})\mathbf{E})$
- 6: Match decoded $\tilde{\mathbf{B}}$ with target watermark \mathbf{B}
- 7: Compute the watermark detection rate $\eta_F = \mathcal{V}_W(\mathbf{W}, \mathbf{B}, \theta)$
- 8: Compute p-value corresponding to the detection rate η_T and η_F

Output: p-value corresponding to the detection rate η_T and η_F .

6 EXPERIMENTAL RESULTS

This section illustrates the empirical study of the proposed FedIPR in terms of *fidelity*, *significance* and *robustness* of watermarks. Superior detection performances of both backdoor-based watermarks and feature-based watermarks in the presence of **Challenge A and B** demonstrate that FedIPR provides a reliable and robust scheme for FedDNN ownership verification.

6.1 Experiment Settings

This subsection illustrates the settings of the empirical study of our FedIPR framework, which is summarized in Tab. 3.

DNN Model Architectures. The deep neural network architectures we investigated include the well-known AlexNet, ResNet-18, and DistilBERT [42]. For convolution neural networks, feature-based binary watermarks are embedded into normalization scale weights \mathbf{W}_γ of multiple convolution layers in AlexNet and ResNet-18; for transformer-based neural networks, feature-based watermarks are embedded into *Layer-Normalization* scale weights \mathbf{W}_γ of multiple encoders in DistilBERT. The detailed model architectures are shown in Appendix C.

Datasets. For image classification tasks, FedIPR is evaluated on CIFAR10 and CIFAR100 datasets, and for natural language processing tasks, FedIPR is evaluated on GLUE benchmark including SST2 and QNLI datasets.

Federated Learning Settings. We simulate a horizontal federated learning setting in which clients upload local models in each communication round, and the server adopts Fedavg [13] algorithm to aggregate the local models. Detailed experimental hyper-parameters to conduct FedIPR are listed in Appendix C. Our source code for implementation will be open-sourced once the paper is accepted.

6.2 Evaluation Metrics

Following previous DNN watermarking methods [5], [7], [12], to measure the *fidelity*, *watermark significance* and *robustness* of the proposed FedIPR framework, we apply a set of metrics as below:

Fidelity. We use classification accuracy on the main task Acc_{main} as the metrics for *fidelity*. It is expected classification accuracy should not be degraded by watermarks embedded in FedDNN (see Sect. 6.3 for experimental results).

Watermark Significance. The *watermark significance* measures the statistical significance that the watermarks can provide to rightfully support the ownership verification. We treat the watermark detection as a hypothesis testing process (illustrated in Algo. 4), the watermark significance is calculated in two phases:

- **Watermark Detection Rate.** In the first phase, the watermark detection could be formulated as a classification problem which returns the watermark detection rate η_T and η_F (defined in Sect. 4.1).
- **Statistical Significance (p-value).** In the second phase, we further adopt the p-value of hypothesis testing to quantify the statistical significance of watermarks.

Robustness. We measure the detection rate and statistical significance of watermarks with/without training strategies and attacks to report the robustness.

6.3 Fidelity

We compare the main task performance Acc_{main} of FedIPR against FedAvg to report the fidelity of the proposed FedIPR.

Architecture	Datasets	Watermarks		Metrics			Freeriders
		Feature-based	Backdoor-based	Fidelity	Significance	Robustness	
AlexNet	CIFAR10	Fig. 8, 9	Tab. 5	Fig. 7	Tab. 4, 6	Fig. 10, 11, 12. Tab. 7, 8, 9	Fig. 13
ResNet18	CIFAR100	Fig. 8	Tab. 5	Fig. 7	Tab. 4, 6	Fig. 10, 11, 12. Tab. 7, 8	Fig. 13
DistilBERT	SST2, QNLI	Fig. 8		Fig. 7	Tab. 4		

TABLE 3: Reported experiment results under different settings for proposed feature-based watermarks and backdoor-based watermarks.

In four different training tasks, varying number (from 10 to 100) of clients may decide to embed different bit-length of backdoor-based watermarks (20 to 100 per client) and feature-based watermarks (50 to 500 bits per client).

Fig. 7 (a)-(d) present the worst drop of classification accuracy Acc_{main} . It is observed that under various watermarking settings, slight model performance drop (not more than 2% as compared with that of $FedAvg$) is observed for four separated tasks.

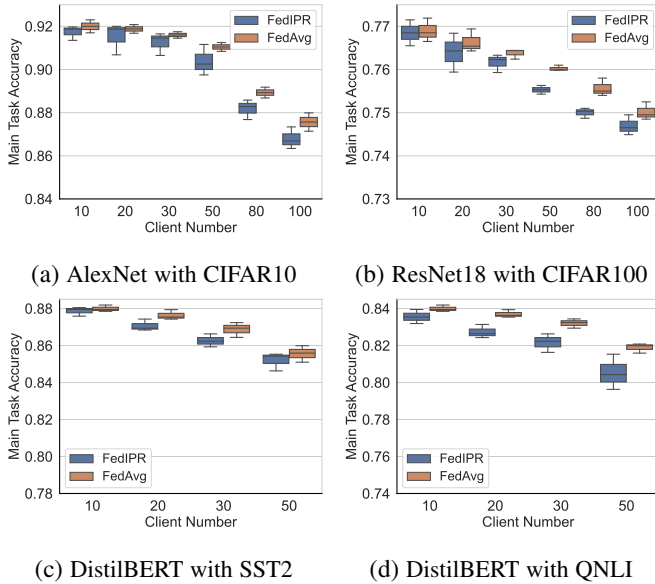


Fig. 7: Figure (a)-(d), respectively, illustrate the main task accuracy Acc_{main} in image and text classification tasks with varying number K of total clients (from 10 to 100), the results are based on cases of varying settings of feature-based and backdoor-based watermarks, the main task accuracy Acc_{main} of FedIPR has slight dropped (not more than 2%) compared to $FedAvg$ scheme.

6.4 Watermark Significance

We present the watermark detection rate and statistical significance to report the watermark significance of the proposed FedIPR framework.

Feature-based Watermarks. Fig. 8 (a)-(d) illustrate feature-based watermark detection rates η_F of varying bit-length of feature-based watermarks, respectively on four different datasets. For convenience, we take that each client in SFL embeds the same length N of watermarks, the significance of feature-based watermarks is as below:

- **Case 1:** As shown in Fig. 8, the detection rate η_F remains constant (100%) within the vertical line (i.e., M/K), where the total bit-length KN assigned by multiple ($K = 5, 10$ or 20) clients does not exceed the capacity of network parameters, which is decided by the channel

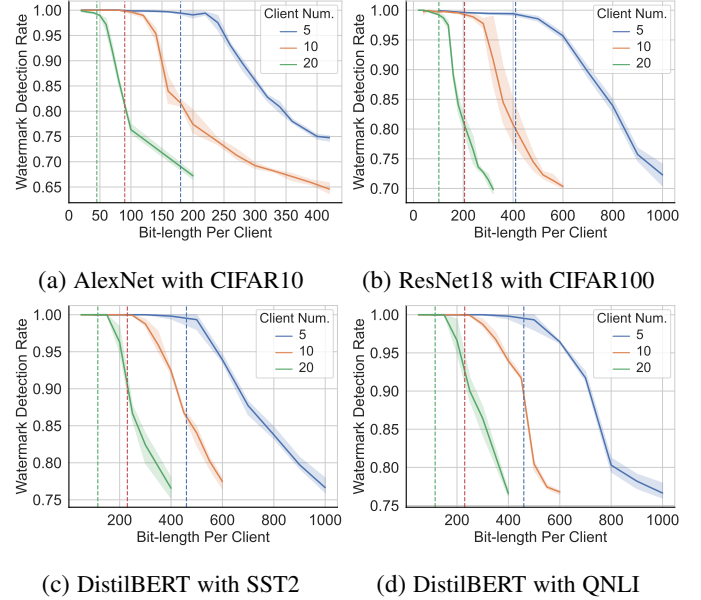


Fig. 8: Figure (a)-(d), respectively, illustrate the feature-based watermark detection rate η_F in image and text classification tasks with varying bit-length per client, in SFL with $K = 5, 10, 20$ clients, the dot vertical line indicates M/K , which is the theoretical bound given by Theorem 1.

number M of parameter $\mathbf{S}(\mathbf{W}) = \mathbf{W}_\gamma$, respectively, e.g., $M = 896$ channels across the last 3 layers for AlexNet and $M = 2048$ channels across the last 4 layers for ResNet18 (illustrated in Appendix C). Therefore, when the total bit-length KN assigned by clients does not exceed the channel number M , almost all bits of feature-based watermarks can be reliably detected, which is in accordance to the Case 1 of Theorem 1⁷.

- **Case 2:** When total length of watermarks KN exceeds the channel number M ($KN > M$), Fig. 9 presents the detection rate η_F drops to about 80% due to the conflicts of overlapping watermark assignments, yet the measured η_F is greater than the lower bound given by Case 2 of Theorem 1 (denoted by the red dot line).

As illustrated in **Case 2**, feature-based watermarks embedded by $K = 5$ clients in SFL may conflict with each other. We give some examples of statistical significance by p-value in Tab. 4, even in the worst case of experiments on four different tasks, the p-value

7. If $KN \leq M$, then there exists \mathbf{W} such that $\eta_F = 1$, the results shown that η_F sometimes goes slightly below the lower bound (100%) provided by Case 1 of Theorem 1. We believe it is because the training is a multi-task optimization process as defined in Eq. (6), watermarking optimization $L_{B,\theta}$ is affected by the main training task optimization L_D , so the solution of watermarking is compromised to maintain the main task performance.

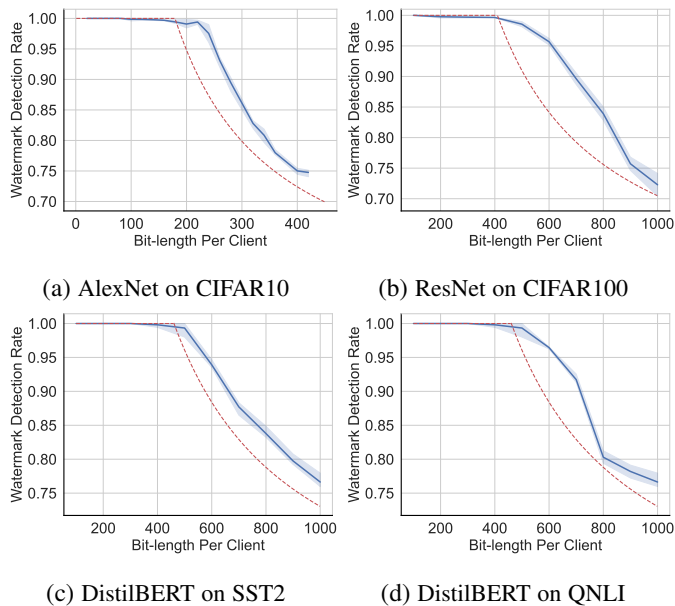


Fig. 9: Figure provides the lower bound (red dot line) of feature-based watermark detection rate η_F given by Theorem 1, and the empirical results (blue line) are demonstrated to be above the theoretical bound (Case 2) in a SFL setting of $K = 5$ clients.

of watermarks is guaranteed below $1.17e-17$, which provides a strong evidence to support claim of ownership.

Task	CIFAR10	CIFAR100	SST2	QNLI
N Per Client	400	400	1000	1000
Detection Rate η_F	75%	71%	76%	75%
p-value	$1.29e-24$	$1.14e-17$	$8.61e-64$	$6.73e-59$

TABLE 4: In the worst case of detection rate, table shows the statistical significance of feature-based watermarks.

Backdoor-based Watermarks. Tab. 5 illustrates the detection rate η_T ⁸ and statistical significance of backdoor-based watermarks, where different number of clients ($K = 5, 10$ or 20) embed backdoor-based watermarks (triggers) generated by Projected Gradient Descent (PGD) method [43]. The results show that the watermark detection rate η_T almost keeps constant even the trigger number per client increases as much as $N_T = 300$. Moreover, detection rate η_T of watermarks embedded in the more complex ResNet18 is as stable as those watermarks embedded in AlexNet. Also, it is noticed that the detection rate is not influenced by the varying number N_T of backdoor samples. We ascribe the stable detection rate η_T to the generalization capability of over-parameterized networks as demonstrated in [44], [45].

While with a large set of backdoor-based watermarks are embedded in FedDNN model, we give some examples of the statistical significance by p-value in Tab. 6. Even if the detection rate is lower than 100%, the p-value of watermarks is guaranteed below $4.02e-142$, which provides a strong evidence to support claim of ownership.

8. The trigger samples are regarded as correctly detected when the designated targeted adversarial labels are returned.

Task	CIFAR10	CIFAR10	CIFAR100	CIFAR100
Client Number K	10	5	10	5
N_T Per Client	300	150	150	100
Detection Rate η_T	97%	98%	98%	98%
p-value	$1.86e-275$	$4.02e-142$	$5.35e-289$	$4.85e-193$

TABLE 6: In the worst cases of detection rate, table shows statistical significance of backdoor-based watermarks.

6.5 Robustness under Federated Learning Strategies

As illustrated in technical **Challenge B** of Sect. 4.3, strategies like differential privacy [38], client selection [13] and defensive aggregation mechanism [21], [22], [23] are widely used for privacy, security and efficiency in secure federated learning. Those strategies intrinsically bring performance decays on the main classification task. Respectively, we evaluate the detection rate η_F and η_T of watermarks under **Challenge B** to report the robustness of FedIPR.

6.5.1 Robustness Against Differential Privacy

We adopt the Gaussian noise-based method to provide differential privacy guarantee for federated learning. Specifically, we vary the standard deviation σ of Gaussian noise on the local models before clients send local models to the server. As Fig. 10 (a)-(b) show, the main task performance Acc_{main} decreases severely as the σ of noise increases, and the feature-based detection rate η_F and backdoor-based detection rate η_T drop a little while the Acc_{main} is within usable range (more than 85%). In a concrete way, when σ equals 0.003, classification accuracy Acc_{main} , detection rate η_F and η_T keep a high performance, which demonstrates the robustness of watermarks under differential privacy strategy.

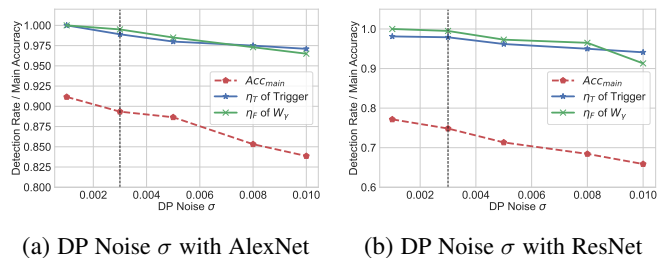


Fig. 10: This figure describes performance of FedIPR under differential privacy strategies using random noise to protect exchanged model information. In a federated learning setting of 10 clients, respectively, figure (a)-(b) illustrate feature-based detection rate η_F and backdoor-based detection rate η_T under varying differential private noise σ , where the dot lines illustrate the main task accuracy Acc_{main} .

We provide some examples of statistical significance by p-value in Tab. 7, even in the worst case of detection rate, the p-value of watermarks is guaranteed below $2.89e-15$, which provides a strong evidence to support claim of ownership.

6.5.2 Robustness Against Client Selection

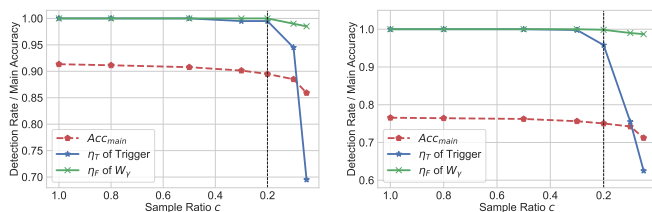
We select cK of K clients ($c < 1$) to participate training in each epoch for communication efficiency. Fig. 11 shows that the watermarks could not be removed even the sample ratio c is as low as 0.25. More specifically, when the sample ratio is larger than 0.2, the main classification accuracy Acc_{main} and detection rate η_T and η_F keep constant. This result gives a lower bound of client sampling rate in which watermarks can be effectively embedded and verified.

Model/Dataset	Client Num.	Trigger sample number N_T per client					
		50	100	150	200	250	300
AlexNet/CIFAR10	20	99.34% \pm 0.31%	99.30% \pm 0.60%	99.35% \pm 0.31%	99.03% \pm 0.57%	99.17% \pm 0.47%	98.85% \pm 0.69%
	10	99.59% \pm 0.23%	98.92% \pm 0.20%	98.45% \pm 0.67%	98.24% \pm 0.57%	98.43% \pm 0.15%	97.56% \pm 1.07%
	5	99.29% \pm 0.38%	99.03% \pm 0.44%	98.15% \pm 0.74%	98.71% \pm 0.43%	98.28% \pm 0.30%	98.39% \pm 0.64%
ResNet18/CIFAR100	20	99.64% \pm 0.31%	99.60% \pm 0.20%	99.35% \pm 0.31%	99.59% \pm 0.46%	99.93% \pm 0.05%	99.92% \pm 0.07%
	10	99.86% \pm 0.05%	99.58% \pm 0.41%	98.56% \pm 0.57%	99.84% \pm 0.04%	99.83% \pm 0.15%	99.88% \pm 0.03%
	5	98.89% \pm 0.80%	98.54% \pm 1.3%	99.07% \pm 2.34%	98.94% \pm 0.73%	99.45% \pm 0.06%	98.44% \pm 0.25%

TABLE 5: Table presents the superior backdoor-based watermark detection rate (above 95%). Respectively, table illustrates η_T of varying bit-length N_T of watermarks, where the datasets investigated include CIFAR10 and CIFAR100 datasets and the client number is 5, 10, 20.

Task	CIFAR10	CIFAR10	CIFAR100	CIFAR100
Watermark Type	Feature	Backdoor	Feature	Backdoor
N/N_T Per Client	80	80	80	80
Detection Rate	96.25%	97.50%	91.25%	93.75%
p-value	7.06e-20	2.56e-75	2.89e-15	2.28e-143

TABLE 7: In the worst case of detection rate, table shows the statistical significance of watermarks under differential privacy strategy using random noise.



(a) Sample Ratio with AlexNet (b) Sample Ratio with ResNet

Fig. 11: Figure describes the robustness of FedIPR under client selection strategy. In a federated learning setting of 10 clients, respectively, figure (a)-(b) illustrate feature-based detection rate η_F and backdoor-based detection rate η_T under different sample ratio c , whereas the dot lines illustrate the main task accuracy Acc_{main} .

We give some examples of statistical significance by p-value in Tab. 8, even in the worst case of detection rate, the p-value of watermarks is guaranteed below $7.02e-20$, which provides a strong evidence to support claim of ownership.

Task	CIFAR10	CIFAR10	CIFAR100	CIFAR100
Watermark Type	Feature	Backdoor	Feature	Backdoor
N/N_T Per Client	80	80	80	80
Detection Rate	97.50%	68.75%	96.25%	62.50%
p-value	2.68e-21	2.74e-36	7.02e-20	6.60e-79

TABLE 8: In the worst case of detection rate, table shows statistical significance of watermarks under client selection strategy.

6.5.3 Robustness Against Defensive Aggregation

Our experiments show that even when defensive methods like Trimmed-Mean, Krum, Bulyan [21], [22], [23] are employed to defense byzantine attacks, backdoor-based watermark detection rates of more than 63.25% can still be maintained, which means a near 100% probability of detected plagiarism is guaranteed with p-value less than $1e^{-30}$. The result is shown in Tab. 9.

While for feature-based watermarks under defensive methods in SFL, as presented in Tab. 10, the detection rate remains above 97%, the p-value of watermarks is guaranteed below $2.68e-21$, which provides a strong evidence to support claim of ownership.

Method	Bulyan	Multi-Krum	Trim-mean	FedAvg
N_T Per Client	80	80	80	80
Detection Rate η_T	68.67%	79.82%	63.25%	98.82%
p-value	5.24e-35	1.74e-47	4.02e-30	7.20e-78

TABLE 9: Statistical significance of backdoor-based watermarks under defensive aggregation, where 10 clients train AlexNet with CIFAR10 dataset.

Method	Bulyan	Multi-Krum	Trim-mean	FedAvg
N Per Client	80	80	80	80
Detection Rate η_F	98.75%	100%	97.5%	100%
p-value	6.61e-23	0	2.68e-21	0

TABLE 10: Statistical significance of feature-based watermarks under defensive aggregation, where 10 clients train AlexNet with CIFAR10 dataset.

6.6 Robustness Against Removal Attack

In this subsection, we showcase that FedIPR are robust against removal attacks conducted by plagiarizers that attempt to remove the watermarks. The feature-based watermarks embedded in normalization layer are shown to be especially persistent against both fine-tuning attack and pruning attack.

6.6.1 Robustness against Fine-tuning Attack

Fine-tuning attack on watermarks is conducted to train the network without the presence of the regularization term, *i.e.*, L_T and $L_{B,\theta}$. In Fig. 12 (a), it is observed that the detection rate η_F of watermarks embedded with normalization layer (\mathbf{W}_γ) remains at 100% (blue curve). In contrast, the detection rate η_F of watermarks embedded with convolution layer (\mathbf{W}_C) drops significantly (purple curve). The superior robustness of feature-based watermarks embedded in normalization layer is in accordance to the observations reported in [35]. While for backdoor-based watermarks, the detection rate η_T remains above 90% (yellow curve), which is also robust against fine-tuning attack.

6.6.2 Robustness against Pruning Attack

The pruning attack removes redundant parameters from the trained model. We evaluate the main task performance Acc_{main} and watermark detection rate η_F and η_T under pruning attack with varying pruning rates. Fig. 12 (b) shows watermark detection rate η_F and η_T while varying proportions of network parameters are pruned. It is observed that the detection rate η_F of watermarks embedded in the normalization layer is stable all the time, while η_F with \mathbf{W}_C are severely degraded. This fact shows that the watermarks on normalization parameters are more robust against pruning attack. While for backdoor-based watermarks, the detection rate η_T remains above 90% (yellow curve) when pruning rate is less than 60%, which is also robust against pruning attack.

		$\beta = 0.1$						
		N Per Client	50	100	200	300	400	500
Resnet	Accuracy Acc_{main}	68.61% \pm 0.14%	68.54% \pm 0.20%	68.33% \pm 0.05%	67.55% \pm 0.07%	67.38% \pm 0.09%	67.33% \pm 0.10%	
	Backdoor-based η_T	99.73% \pm 0.14%	99.74% \pm 0.24%	99.85% \pm 0.13%	99.75% \pm 0.23%	99.73% \pm 0.19%	99.69% \pm 0.13%	
	Feature-based η_F	100.0% \pm 0%	99.73% \pm 0.25%	99.90% \pm 0.05%	98.96% \pm 0.76%	81.83% \pm 1.38%	78.45% \pm 0.68%	
			$\beta = 1.0$					
		N Per Client	50	100	200	300	400	500
		Accuracy Acc_{main}	74.52% \pm 0.23%	74.48% \pm 0.33%	74.64% \pm 0.05%	73.96% \pm 0.35%	73.81% \pm 0.13%	73.31% \pm 0.06%
	Backdoor-based η_T	99.85% \pm 0.14%	99.85% \pm 0.15%	99.74% \pm 0.24%	99.75% \pm 0.23%	0.9974 \pm 0.23%	0.9973 \pm 0.13%	
	Feature-based η_F	100% \pm 0%	99.60% \pm 0.10%	99.55% \pm 0.05%	97.66% \pm 0.73%	80.87% \pm 1.53%	77.97% \pm 0.53%	
Alexnet			$\beta = 0.1$					
		N Per Client	50	100	150	200	250	300
		Accuracy Acc_{main}	82.30% \pm 0.31%	82.52% \pm 0.60%	82.65% \pm 0.19%	82.42% \pm 1.02%	81.49% \pm 0.85%	81.38% \pm 0.93%
		Backdoor-based η_T	99.24% \pm 0.25%	99.30% \pm 0.21%	99.53% \pm 0.15%	99.82% \pm 0.13%	99.81% \pm 0.09%	99.82% \pm 0.13%
		Feature-based η_F	100% \pm 0%	99.84% \pm 0.08%	93.49% \pm 0.40%	86.87% \pm 0.31%	79.87% \pm 0.51%	76.97% \pm 0.43%
			$\beta = 1.0$					
		N Per Client	50	100	150	200	250	300
		Accuracy Acc_{main}	89.76% \pm 0.09%	89.50% \pm 0.07%	89.46% \pm 0.21%	88.53% \pm 0.23%	88.60% \pm 0.13%	88.43% \pm 0.34%
		Backdoor-based η_T	99.25% \pm 0.25%	99.34% \pm 0.46%	99.54% \pm 0.23%	99.85% \pm 0.15%	99.75% \pm 0.31%	99.75% \pm 0.31%
		Feature-based η_F	99.80% \pm 0.20%	99.61% \pm 0.13%	94.24% \pm 0.13%	87.14% \pm 0.38%	77.14% \pm 0.48%	75.36% \pm 0.68%

TABLE 11: Table illustrates the watermark detection rate η_T , η_F and main accuracy Acc_{main} in a non-iid federated learning setting, of image classification tasks including AlexNet on CIFAR10 dataset and ResNet on CIFAR100 dataset. $K = 10$ clients embed feature-based and backdoor-based watermarks, with varying feature-based watermark length N per client, the trigger number is set to 80. The results including non-iid settings sampled from dirichlet distribution with $\beta = 0.1$ and 1.

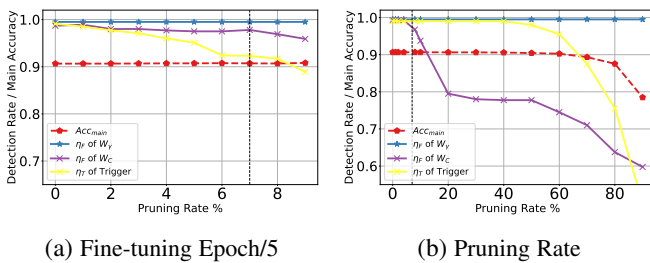


Fig. 12: Figure describes the robustness of our FedIPR under removal attacks. In a federated learning setting, $K = 10$ clients train AlexNet with CIFAR10 dataset. The dot lines in figure (a) and (b) illustrate the main task classification accuracy Acc_{main} under diverse settings. Respectively, figure (a) illustrates feature-based and backdoor-based watermark detection rate against model finetuning attack in 50 epochs; figure (b) illustrates feature-based and backdoor-based watermark detection rate against model pruning attack with varying pruning rate. Note that detection rates η_F of feature-based watermarks in both normalization layer (W_γ) and convolution layer (W_C) are investigated.

6.7 Robustness under Non-iid Setting

In federated learning, data distributions across clients are often not identical and independent distributed (iid). We also evaluate FedIPR in *table-skew* non-iid federated learning setting, where we assume each client’s training examples are drawn with class labels following a *dirichlet distribution* [46], $\beta > 0$ is the concentration parameter controlling the identicalness among users.

In our experiments, we conduct image classification experiments with AlexNet on CIFAR10 and ResNet on CIFAR100, the dirichlet parameter is $\beta = 0.1$ and 1. The results presented in Tab. 11 indicate that FedIPR works with non-iid setting.

In non-iid setting, while a large set of feature-based watermarks are embedded in FedDNN model, we give some examples of statistical significance by p-value in the worst case of detection rate in Tab. 12.

Task	CIFAR10	CIFAR10	CIFAR100	CIFAR100
Non-iid β	0.1	1	0.1	1
N Per Client	300	300	500	500
Detection Rate η_F	76%	75%	78%	77%
p-value	2.42e-20	7.16e-19	4.76e-38	2.33e-35

TABLE 12: In the worst case of detection rate, table shows the statistical significance of watermarks under non-iid SFL.

As shown in Tab. 12, even in the worst case, the p-value of watermarks can be guaranteed below 7.16e-19, which provides a strong evidence to support claim of ownership.

6.8 Watermarks Defeat Freerider Attacks

As a precaution method for freerider attack, watermarks are embedded into the FedDNN, the benign clients can verify ownership by extracting predefined watermarks from FedDNN, while freeriders can not detect watermarks because they do not perform actual training. We conduct experiments testing the local models by three types of clients including plain freerider, freerider with Gaussian noise (defined in Sect. 3.2) and benign clients that contribute data and computation.

We consider a setting that the server conducts feature-based verification on each client’s local models, in a 22-clients federated learning including one freerider client with Gaussian noise and one plain freerider client with previous local models. In each communication round, the results are presented in Fig. 13, which show that the server can detect the benign clients’ watermarks in the global model at quite early stage (in 30 communication rounds) of FedDNN model training, the watermark detection rate η_F is nearly 100%; while the freeriders failed to verify their watermarks because they do not contribute actual training, the η_F detection rate is an almost random guess (50%).

7 CONCLUSION

This paper presents a novel ownership verification scheme to protect the Intellectual Property Right (IPR) of Federated DNN models

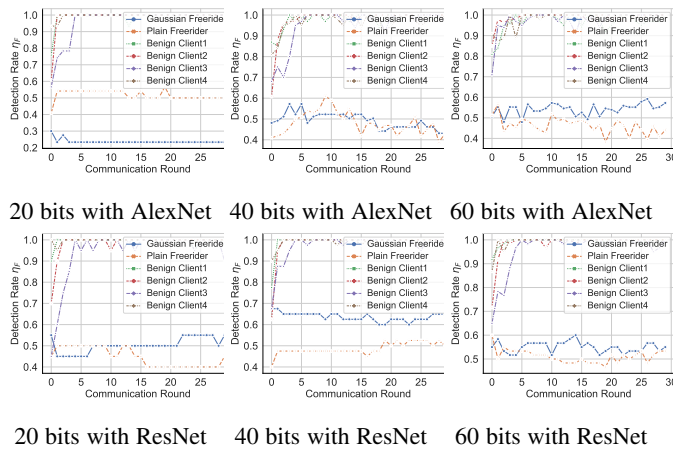


Fig. 13: Comparisons between three different types of clients including: (1) freerider clients with previous local models. (orange lines) (2) freerider clients disguised with Gaussian noise. (blue lines) (3) four benign clients in a 20 client SFL. The feature-based watermark detection rate η_F is measured in each communication round. Note the sharp contrast of η_F between four benign clients and two freerider clients (plotted in orange and blue).

against external plagiarizers who illegally copy, re-distribute the models. To our best knowledge, it is the first ownership verification scheme that aims to protect model intellectual property rights under secure federated learning setting. This work addresses a crucial issue remained open in secure federated learning research, since the protection of valuable federated learning models is as important as protecting data privacy.

On the technical side, this work demonstrates that reliable and persistent watermarks could be embedded into local models without disclosing the presence and extraction parameters of these watermarks. In particular, normalization scale parameters based on watermarks are extremely robust under federated learning strategies and against removal attacks. We wish that the formulation illustrated in this paper will lead to watermark embedding and verification in various federated learning settings.

ACKNOWLEDGMENTS

This research is partly supported by National Key Research and Development Program of China (2020YFB1805501, 2018AAA0101100 and 2020YFB1806700), NSFC Grant 61932014 and Project BE2020026 supported by the Key Research and Development Program of Jiangsu, China.

REFERENCES

- [1] J. Deng, W. Dong, R. Socher, L.-J. Li, K. Li, and L. Fei-Fei, "Imagenet: A large-scale hierarchical image database," in *2009 IEEE conference on computer vision and pattern recognition*. Ieee, 2009, pp. 248–255.
- [2] C. Wang, M. Riviere, A. Lee, A. Wu, C. Talnikar, D. Haziza, M. Williamson, J. Pino, and E. Dupoux, "Voxpopuli: A large-scale multilingual speech corpus for representation learning, semi-supervised learning and interpretation," in *Proceedings of the 59th Annual Meeting of the Association for Computational Linguistics and the 11th International Joint Conference on Natural Language Processing (Volume 1: Long Papers)*, 2021, pp. 993–1003.
- [3] C. Chelba, T. Mikolov, M. Schuster, Q. Ge, T. Brants, P. Koehn, and T. Robinson, "One billion word benchmark for measuring progress in statistical language modeling," *arXiv preprint arXiv:1312.3005*, 2013.
- [4] Y. Zhu, R. Kiros, R. Zemel, R. Salakhutdinov, R. Urtasun, A. Torralba, and S. Fidler, "Aligning books and movies: Towards story-like visual explanations by watching movies and reading books," in *Proceedings of the IEEE international conference on computer vision*, 2015, pp. 19–27.

- [5] L. Fan, K. W. Ng, C. S. Chan, and Q. Yang, "Deepip: Deep neural network intellectual property protection with passports," *IEEE Transactions on Pattern Analysis and Machine Intelligence*, 2021.
- [6] D. S. Ong, C. S. Chan, K. W. Ng, L. Fan, and Q. Yang, "Protecting intellectual property of generative adversarial networks from ambiguity attack," in *Proceedings of the IEEE/CVF Conference on Computer Vision and Pattern Recognition (CVPR)*, 2021.
- [7] J. Zhang, D. Chen, J. Liao, W. Zhang, H. Feng, G. Hua, and N. Yu, "Deep model intellectual property protection via deep watermarking," *IEEE Transactions on Pattern Analysis and Machine Intelligence*, 2021.
- [8] J. H. Lim, C. S. Chan, K. W. Ng, L. Fan, and Q. Yang, "Protect, show, attend and tell: Empowering image captioning models with ownership protection," *Pattern Recognition*, vol. 122, p. 108285, 2022.
- [9] Y. Uchida, Y. Nagai, S. Sakazawa, and S. Satoh, "Embedding watermarks into deep neural networks," in *Proceedings of the 2017 ACM on International Conference on Multimedia Retrieval*, 2017, pp. 269–277.
- [10] H. Chen, B. Darvish Rohani, and F. Koushanfar, "DeepMarks: A Digital Fingerprinting Framework for Deep Neural Networks," *arXiv e-prints*, p. arXiv:1804.03648, Apr. 2018.
- [11] B. Darvish Rouhani, H. Chen, and F. Koushanfar, "DeepSigns: A Generic Watermarking Framework for IP Protection of Deep Learning Models," *arXiv e-prints*, p. arXiv:1804.00750, Apr. 2018.
- [12] Y. Adi, C. Baum, M. Cisse, B. Pinkas, and J. Keshet, "Turning your weakness into a strength: Watermarking deep neural networks by backdooring," in *27th USENIX Security Symposium (USENIX)*, 2018.
- [13] B. McMahan, E. Moore, D. Ramage, S. Hampson, and B. A. y Arcas, "Communication-Efficient Learning of Deep Networks from Decentralized Data," in *Proceedings of the 20th International Conference on Artificial Intelligence and Statistics*, ser. Proceedings of Machine Learning Research, A. Singh and J. Zhu, Eds., vol. 54. Fort Lauderdale, FL, USA: PMLR, 20–22 Apr 2017, pp. 1273–1282. [Online]. Available: <http://proceedings.mlr.press/v54/mcmahan17a.html>
- [14] Q. Yang, Y. Liu, T. Chen, and Y. Tong, "Federated machine learning: Concept and applications," *ACM Transactions on Intelligent Systems and Technology (TIST)*, vol. 10, no. 2, p. 12, 2019.
- [15] P. Kairouz, H. B. McMahan, B. Avent, A. Bellet, M. Bennis, A. N. Bhagoji, K. Bonawitz, Z. Charles, G. Cormode, R. Cummings, R. G. L. D'Oliveira, S. E. Rouayheb, D. Evans, J. Gardner, Z. Garrett, A. Gascón, B. Ghazi, P. B. Gibbons, M. Gruteser, Z. Harchaoui, C. He, L. He, Z. Huo, B. Hutchinson, J. Hsu, M. Jaggi, T. Javidi, G. Joshi, M. Khodak, J. Konečný, A. Korolova, F. Koushanfar, S. Koyejo, T. Lepoint, Y. Liu, P. Mittal, M. Mohri, R. Nock, A. Özgür, R. Pagh, M. Raykova, H. Qi, D. Ramage, R. Raskar, D. Song, W. Song, S. U. Stich, Z. Sun, A. T. Suresh, F. Tramèr, P. Vepakomma, J. Wang, L. Xiong, Z. Xu, Q. Yang, F. X. Yu, H. Yu, and S. Zhao, "Advances and open problems in federated learning," *Foundations and Trends® in Machine Learning*, vol. abs/1912.04977, 2019. [Online]. Available: <http://arxiv.org/abs/1912.04977>
- [16] L. Zhu, Z. Liu, and S. Han, "Deep leakage from gradients," in *NeurIPS*, H. M. Wallach, H. Larochelle, A. Beygelzimer, F. d'Alché-Buc, E. B. Fox, and R. Garnett, Eds., 2019, pp. 14 747–14 756. [Online]. Available: <http://papers.nips.cc/paper/9617-deep-leakage-from-gradients>
- [17] X. Luo, Y. Wu, X. Xiao, and B. C. Ooi, "Feature inference attack on model predictions in vertical federated learning," in *2021 IEEE 37th International Conference on Data Engineering (ICDE)*. IEEE, 2021, pp. 181–192.
- [18] L. T. Phong, Y. Aono, T. Hayashi, L. Wang, and S. Moriai, "Privacy-preserving deep learning via additively homomorphic encryption," *IEEE Transactions on Information Forensics and Security*, vol. 13, no. 5, pp. 1333–1345, 2018.
- [19] M. Abadi, A. Chu, I. Goodfellow, H. B. McMahan, I. Mironov, K. Talwar, and L. Zhang, "Deep learning with differential privacy," in *Proceedings of the 2016 ACM SIGSAC Conference on Computer and Communications Security*, 2016, pp. 308–318.
- [20] T. Ryffel, D. Pointcheval, and F. R. Bach, "ARIANN: low-interaction privacy-preserving deep learning via function secret sharing," *CoRR*, vol. abs/2006.04593, 2020. [Online]. Available: <https://arxiv.org/abs/2006.04593>
- [21] P. Blanchard, E. M. El Mhamdi, R. Guerraoui, and J. Stainer, "Machine learning with adversaries: Byzantine tolerant gradient descent," in *Proceedings of the 31st International Conference on Neural Information Processing Systems*, 2017, pp. 118–128.
- [22] R. Guerraoui, S. Rouault *et al.*, "The hidden vulnerability of distributed learning in byzantium," in *International Conference on Machine Learning*. PMLR, 2018, pp. 3521–3530.
- [23] D. Yin, Y. Chen, R. Kannan, and P. Bartlett, "Byzantine-robust distributed

- learning: Towards optimal statistical rates,” in *International Conference on Machine Learning*. PMLR, 2018, pp. 5650–5659.
- [24] Y. Fraboni, R. Vidal, and M. Lorenzi, “Free-rider attacks on model aggregation in federated learning,” in *International Conference on Artificial Intelligence and Statistics*. PMLR, 2021, pp. 1846–1854.
- [25] J. Lin, M. Du, and J. Liu, “Free-riders in federated learning: Attacks and defenses,” *arXiv preprint arXiv:1911.12560*, 2019.
- [26] L. Lyu, H. Yu, and Q. Yang, “Threats to federated learning: A survey,” *arXiv preprint arXiv:2003.02133*, 2020.
- [27] F. Boenisch, “A survey on model watermarking neural networks,” 2020.
- [28] R. Shokri and V. Shmatikov, “Privacy-preserving deep learning,” in *Proceedings of the 22nd ACM SIGSAC conference on computer and communications security*, 2015, pp. 1310–1321.
- [29] M. de Boer, “Ai as a target and tool: An attacker’s perspective on ml,” 2020. [Online]. Available: <https://www.gartner.com/en/documents/3939991>
- [30] F. Tramèr, F. Zhang, A. Juels, M. K. Reiter, and T. Ristenpart, “Stealing machine learning models via prediction {APIs};” in *25th USENIX security symposium (USENIX Security 16)*, 2016, pp. 601–618.
- [31] T. Orekondy, B. Schiele, and M. Fritz, “Knockoff nets: Stealing functionality of black-box models,” in *Proceedings of the IEEE/CVF Conference on Computer Vision and Pattern Recognition*, 2019, pp. 4954–4963.
- [32] J. Zhang, Z. Gu, J. Jang, H. Wu, M. P. Stoecklin, H. Huang, and I. Molloy, “Protecting intellectual property of deep neural networks with watermarking,” in *Proceedings of the 2018 on Asia Conference on Computer and Communications Security (ASIACCS)*, 2018, pp. 159–172.
- [33] N. Lukas, Y. Zhang, and F. Kerschbaum, “Deep neural network fingerprinting by conferrable adversarial examples,” in *International Conference on Learning Representations*, 2020.
- [34] J. Zhang, D. Chen, J. Liao, W. Zhang, G. Hua, and N. Yu, “Passport-aware normalization for deep model protection,” in *Advances in Neural Information Processing Systems*, H. Larochelle, M. Ranzato, R. Hadsell, M. F. Balcan, and H. Lin, Eds., vol. 33. Curran Associates, Inc., 2020, pp. 22 619–22 628. [Online]. Available: <https://proceedings.neurips.cc/paper/2020/file/ff1418e8cc993fe8abcfe3ce2003e5c5-Paper.pdf>
- [35] L. Fan, K. W. Ng, and C. S. Chan, “Rethinking deep neural network ownership verification: Embedding passports to defeat ambiguity attacks,” in *Advances in Neural Information Processing Systems*. Curran Associates, Inc., 2019, pp. 4714–4723.
- [36] B. G. Atli, Y. Xia, S. Marchal, and N. Asokan, “Waffle: Watermarking in federated learning,” *arXiv preprint arXiv:2008.07298*, 2020.
- [37] Z. Sun, P. Kairouz, A. Theertha Suresh, and H. B. McMahan, “Can You Really Backdoor Federated Learning?” *arXiv e-prints*, p. arXiv:1911.07963, Nov. 2019.
- [38] K. Wei, J. Li, M. Ding, C. Ma, H. H. Yang, F. Farokhi, S. Jin, T. Q. Quek, and H. V. Poor, “Federated learning with differential privacy: Algorithms and performance analysis,” *IEEE Transactions on Information Forensics and Security*, vol. 15, pp. 3454–3469, 2020.
- [39] E. Bagdasaryan, A. Veit, Y. Hua, D. Estrin, and V. Shmatikov, “How to backdoor federated learning,” *arXiv preprint arXiv:1807.00459*, 2018.
- [40] A. Madry, A. Makelov, L. Schmidt, D. Tsipras, and A. Vladu, “Towards deep learning models resistant to adversarial attacks,” *arXiv preprint arXiv:1706.06083*, 2017.
- [41] A. Vaswani, N. Shazeer, N. Parmar, J. Uszkoreit, L. Jones, A. N. Gomez, Ł. Kaiser, and I. Polosukhin, “Attention is all you need,” *Advances in neural information processing systems*, vol. 30, 2017.
- [42] V. Sanh, L. Debut, J. Chaumond, and T. Wolf, “Distilbert, a distilled version of bert: smaller, faster, cheaper and lighter,” *arXiv preprint arXiv:1910.01108*, 2019.
- [43] A. Nguyen, J. Yosinski, and J. Clune, “Deep neural networks are easily fooled: High confidence predictions for unrecognizable images,” in *Proceedings of the IEEE conference on computer vision and pattern recognition*, 2015, pp. 427–436.
- [44] Z. Allen-Zhu, Y. Li, and Z. Song, “A convergence theory for deep learning via over-parameterization,” *CoRR*, vol. abs/1811.03962, 2018.
- [45] C. Zhang, S. Bengio, M. Hardt, B. Recht, and O. Vinyals, “Understanding deep learning requires rethinking generalization,” in *ICLR*. OpenReview.net, 2017.
- [46] Q. Li, Y. Diao, Q. Chen, and B. He, “Federated learning on non-iid data silos: An experimental study,” *arXiv preprint arXiv:2102.02079*, 2021.
- [47] N. Alon and K. A. Berman, “Regular hypergraphs, gordon’s lemma, steinitz’ lemma and invariant theory,” *Journal of Combinatorial Theory, Series A*, vol. 43, no. 1, pp. 91–97, 1986.

APPENDIX A PROOF OF THEOREM 1

Definition 1. For $\{\theta_k\}_{k=1}^K$ of K clients, the embedding matrix $\{\mathbf{E}_k\}_{k=1}^K \in \{\theta_k\}_{k=1}^K$ form a combined matrix

$$\mathbf{U}^{M \times KN} = \{\mathbf{E}_1^{M \times N}, \mathbf{E}_2^{M \times N}, \dots, \mathbf{E}_K^{M \times N}\}, \quad (1)$$

where M denotes the channel number of targeted watermark parameters $\mathbf{W} \in \mathbb{R}^M$. Let $\tilde{\mathbf{U}}^{M \times KN}$ be matrix combined with

$$\{(\mathbf{E}_1 \text{diag}(\mathbf{B}_1))^{M \times N}, (\mathbf{E}_2 \text{diag}(\mathbf{B}_2))^{M \times N}, \dots, (\mathbf{E}_K \text{diag}(\mathbf{B}_K))^{M \times N}\}, \quad (2)$$

where $\mathbf{B}_k = (t_{k1}, t_{k2}, \dots, t_{kN}) \in \{+1, -1\}^N$ is the watermark of k -th client.

The detection rate of feature-based watermark could be defined as:

Definition 2. Detection Rate Defined by Matrix

Let $\#\{\mathbf{W}^T \mathbf{A} > 0\}$ be the number of positive elements of $\mathbf{W}^T \mathbf{A}$, for any matrix $\mathbf{W}^T \mathbf{A}$, for any matrix $\mathbf{A} \in \mathbb{R}^{M \times KN}$ and vector $\mathbf{W}^{M \times 1}$.

$$\eta_F = \mathbb{E}_{\tilde{\mathbf{U}}}(\sup_{\mathbf{W} \in \mathbb{R}^M} \#\{\mathbf{W}^T \tilde{\mathbf{U}} > 0\}) / KN. \quad (3)$$

Remark: the Def. 2 provides an explanation of the average form of detection rate η_F (defined in Eq. (8) of main text) with respect to the embedding matrix \mathbf{U} .

Remark: the domain of \mathbf{W} in Def. 2 and following analysis we consider is total space \mathbb{R}^M for parameter \mathbf{W} , which does not consider the influence of optimization process L_D . Optimization process of main task L_D may lead parameters \mathbf{W} to converge in a subspace of total space.

The following Theorem 1 first elucidates the condition under which a feasible solution exists for K different watermarks embedding. Moreover, if the condition is not satisfied, the theorem 1 provides the lower bound of detecting rate η_F of feature-based watermarks.

Theorem 1. Taking \mathbf{U} , $\tilde{\mathbf{U}}$ and η_F defined above, if \mathbf{U} is column (line) non-singular matrix,

Case 1: If $\text{rank}(\mathbf{U}) = KN \leq M$, then there exists \mathbf{W} such that $\mathbf{W}^T \tilde{\mathbf{U}} \geq 0$. Moreover, we have

$$\eta_F = 1 \quad (4)$$

Case 2: If $\text{rank}(\mathbf{U}) = M < KN$, then, we have,

$$\eta_F \geq \frac{KN + M}{2KN}. \quad (5)$$

Proof. For the **Case 1**, if $\text{rank}(\mathbf{U}) = KN$, then the column of \mathbf{U} (U_1, U_2, \dots, U_{KN}) is independent, and the column of $\tilde{\mathbf{U}}$ ($\tilde{U}_1, \tilde{U}_2, \dots, \tilde{U}_{KN}$) is also independent. Thus,

$$\begin{aligned} y_1 \tilde{U}_1 + y_2 \tilde{U}_2 + \dots + y_{KN} \tilde{U}_{KN} &= 0 \\ \iff y_1 = y_2 = \dots = y_{KN} &= 0 \end{aligned} \quad (6)$$

Therefore the solution of $\tilde{\mathbf{U}}\vec{y} = \vec{0}$ is only $\vec{0}$, moreover, $\tilde{\mathbf{U}}\vec{y} = \vec{0}$ doesn't have non-negative solutions except $\vec{0}$. According to Gordan's theorem [47], Either $\tilde{\mathbf{U}}\vec{y} > 0$ has a solution y , or $\tilde{\mathbf{U}}\vec{y} = \vec{0}$ has a nonzero solution y with $\vec{y} \geq \vec{0}$. Since the latter statement

is wrong, there exists $\mathbf{W} = \vec{y}^T$ such that $\mathbf{W}\tilde{\mathbf{U}} > 0$. Therefore, $\eta_F \geq 1$. And since $\eta_F \leq 1$, we have

$$\eta_F = 1 \quad (7)$$

For the **Case 2** as $\text{rank}(\mathbf{U}) = M \leq KN$, since $\tilde{\mathbf{U}} = (U_1 \text{diag}(\mathbf{B}_1), U_2 \text{diag}(\mathbf{B}_2), \dots, U_{KN} \text{diag}(\mathbf{B}_{KN}))$, where $\mathbf{B}_i \in \{-1, 1\}$, $1 \leq i \leq KN$, $\text{rank}(\tilde{\mathbf{B}}) = \text{rank}(\mathbf{B}) = M < KN$.

Without loss of generality, we assume there is a partition of $\tilde{\mathbf{U}}$ as $\tilde{\mathbf{U}} = (\tilde{\mathbf{U}}'_1, \tilde{\mathbf{U}}'_2)$, where $\tilde{\mathbf{U}}'_1 \in \mathbb{R}^{M \times M}$, $\tilde{\mathbf{U}}'_2 \in \mathbb{R}^{M \times KN-M}$ and $\text{rank}(\tilde{\mathbf{U}}'_1) = M$. Denote $\Omega = \{x \in \mathbb{R}^M | x^T \tilde{\mathbf{U}}'_1 > 0\}$ for any $\tilde{\mathbf{U}}'_1$, thus

$$\begin{aligned} &\mathbb{E}_{\tilde{\mathbf{U}}} \sup_x \#\{x^T \tilde{\mathbf{U}} > 0\} \\ &= \mathbb{E}_{(\tilde{\mathbf{U}}'_1, \tilde{\mathbf{U}}'_2)} \sup_{x \in \mathbb{R}^M} (\#\{x^T \tilde{\mathbf{U}}'_1 > 0\} + \#\{x^T \tilde{\mathbf{U}}'_2 > 0\}) \\ &\geq \mathbb{E}_{(\tilde{\mathbf{U}}'_1, \tilde{\mathbf{U}}'_2)} \sup_{x \in \Omega} (\#\{x^T \tilde{\mathbf{U}}'_1 > 0\} + \#\{x^T \tilde{\mathbf{U}}'_2 > 0\}) \\ &= M + \mathbb{E}_{\tilde{\mathbf{U}}'_2} \sup_{x \in \Omega} \#\{x^T \tilde{\mathbf{U}}'_2 > 0\}. \end{aligned} \quad (8)$$

The last inequality is because $x^T \tilde{\mathbf{U}}'_1 > 0$ when $x \in \Omega$. So $\#\{x^T \tilde{\mathbf{U}}'_1 > 0\} = M$.

Since $\tilde{\mathbf{U}}'_2$ is independent of $\tilde{\mathbf{U}}'_1$,

$$\begin{aligned} &\mathbb{E}_{\tilde{\mathbf{U}}'_2} \sup_{x \in \Omega} \#\{x^T \tilde{\mathbf{U}}'_2 > 0\} \\ &= \frac{1}{2} [\mathbb{E}_{\tilde{\mathbf{U}}'_2} \sup_{x \in \Omega} \#\{x^T \tilde{\mathbf{U}}'_2 > 0\} + \mathbb{E}_{-\tilde{\mathbf{U}}'_2} \sup_{x \in \Omega} \#\{x^T \tilde{\mathbf{U}}'_2 > 0\}] \\ &= \frac{1}{2} [\mathbb{E}_{\tilde{\mathbf{U}}'_2} \sup_{x \in \Omega} \#\{x^T \tilde{\mathbf{U}}'_2 > 0\} + \mathbb{E}_{\tilde{\mathbf{U}}'_2} \sup_{x \in \Omega} \#\{x^T \tilde{\mathbf{U}}'_2 < 0\}]. \end{aligned} \quad (9)$$

Consequently,

$$\begin{aligned} &\mathbb{E}_{\tilde{\mathbf{U}}'_2} \sup_{x \in \Omega} \#\{x^T \tilde{\mathbf{U}}'_2 > 0\} \\ &= \frac{1}{2} [\mathbb{E}_{\tilde{\mathbf{U}}'_2} (\sup_{x \in \Omega} \#\{x^T \tilde{\mathbf{U}}'_2 > 0\} + \sup_{x \in \Omega} \#\{x^T \tilde{\mathbf{U}}'_2 < 0\})] \\ &\geq \frac{1}{2} [\mathbb{E}_{\tilde{\mathbf{U}}'_2} (\mathbb{E}_{x \in \Omega} \#\{x^T \tilde{\mathbf{U}}'_2 > 0\} + \mathbb{E}_{x \in \Omega} \#\{x^T \tilde{\mathbf{U}}'_2 < 0\}) \\ &\quad + \mathbb{E}_{x \in \Omega} \#\{x^T \tilde{\mathbf{U}}'_2 = 0\} - \mathbb{E}_{x \in \Omega} \#\{x^T \tilde{\mathbf{U}}'_2 = 0\}] \\ &\geq \frac{1}{2} [\mathbb{E}_{\tilde{\mathbf{U}}'_2} \mathbb{E}_{x \in \Omega} \#\{x^T \tilde{\mathbf{U}}'_2 \in R^{KN-M}\} - \mathbb{E}_{\tilde{\mathbf{U}}'_2} \mathbb{E}_{x \in \Omega} \#\{x^T \tilde{\mathbf{U}}'_2 = 0\}] \\ &= \frac{1}{2} (KN - M). \end{aligned} \quad (10)$$

The last equation because $\mathbb{E}_{\tilde{\mathbf{U}}'_2 \in \mathbb{R}^{M \times KN-M}} \#\{x^T \tilde{\mathbf{U}}'_2 = 0\} = 0$ for any nonzero vector x . Finally, according to Eq. (8) and (10), we have:

$$\begin{aligned} &\mathbb{E}_{\tilde{\mathbf{U}}} \sup_{x \in \mathbb{R}^M} \#\{x^T \tilde{\mathbf{U}} > 0\} \\ &\geq M + \frac{1}{2} (KN - M) \\ &= \frac{1}{2} (KN + M) \end{aligned} \quad (11)$$

Therefore,

$$\eta_F = \mathbb{E}_{\tilde{\mathbf{U}}} \sup_{x \in \mathbb{R}^M} \#\{x^T \tilde{\mathbf{U}} > 0\} \geq \frac{KN + M}{2KN}. \quad (12)$$

□

APPENDIX B HYPOTHESIS TESTING DETAILS

Note that both case 1 and 2 in Theorem 1 analyze the "existence" of model W that ensures the *level of conflicts* between different watermarks is bounded. Corresponding watermark detection rates η_F are thus lower bounded. However, other factors may influence η_F . For example, random noise added to the federated learning process or removal attacks launched by plagiarizers, all conspire to degrade η_F to various extents. Taking these realistic issues into account, we illustrate below how to estimate the optimal bit-length assigned to multiple watermarks under different situations.

Hypothesis Testing. We treat both feature-based and backdoor-based watermark detection as a hypothesis testing process, where \mathcal{H}_0 is "the model is not an (illegal) copy of the model owned by its claimed owner" versus \mathcal{H}_1 "model is an (illegal) copy". Under hypothesis \mathcal{H}_0 , given N bit-length watermark, the event that the model output the right watermark for each bit follows the binomial distribution $B(N, 1/C)$, where C is the class number of the task. **Optimal bit-length and maximal bit-length N .** For **case 1** of Theorem 1, we take the watermark detection rate η_F as a constant which is independent of the bit-length of assigned watermarks, thus the upper bound of p-value is:

$$p\text{-value} \leq \sum_{i=\eta_0 N}^N \binom{N}{i} (1/C)^i (1 - 1/C)^{N-i}, N < M/K, \quad (13)$$

in which $C = 2$. The p-value is a *monotonically decreasing* function of the bit-length N of watermarks. Therefore, the optimal bit-length $N = M/K$ in this case.

For **case 2** of Theorem 1, we take η_F as a function inversely proportional to the bit-length N , thus the upper bound of p-value:

$$p\text{-value} \leq \sum_{i=\frac{KN+M}{2K}}^N \binom{N}{i} (1/C)^i (1 - 1/C)^{N-i}, N \geq M/K, \quad (14)$$

which *monotonically increases* with the bit-length N of watermarks. To sum up, the optimal bit-length for the smallest p-value is

$$N_{opt} = M/K, \quad (15)$$

which provides the most significant watermark verification.

In case p-value is only required to be less than statistical significance level α e.g. 0.0001, we can determine the range of bit-length N that fulfill the requirement. For example in Fig. 1, if $K = 10$ clients decide to embed watermarks into $M = 896$ channels of model parameters, $N_{opt} = 90$, when $\alpha = 0.0001$, the corresponding N_{max} is 550 and N_{min} is 18.

In short, Theorem 1 specifies *the optimal bit-length* and *the acceptable range of watermark bit-length* that allows reliable detection rates with sufficient significance to support ownership verification.

p-value of backdoor-based watermark. The statistical significance can also be adopted to evaluate the significance of backdoor-based watermark.

Under hypothesis \mathcal{H}_0 , given N trigger-set samples, the event that the model \mathbb{N} output the right label y^T of x^T follows the binomial distribution $B(N, 1/C)$, where C is the class number of the task. The p-value is the probability of classifying at least $\eta_T N$ samples correctly

$$p\text{-value} = \sum_{i=\eta_T N}^N \binom{N}{i} (1/C)^i (1 - 1/C)^{N-i}. \quad (16)$$

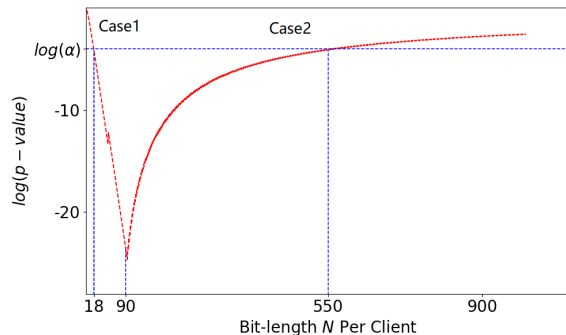


Fig. 1: *The optimal bit-length and the acceptable range of watermark bit-length* that provide strong confidence of ownership verification. As shown in figure, $K = 10, M = 896$, we take $\eta_F = 0.98$ in case 1, the optimal bit-length for p-value is $N_{opt} = M/K = 90$, for an acceptable level $\alpha = 0.0001$, the acceptable range of watermark bit-length is from $N = 18$ to $N = 550$.

APPENDIX C EXPERIMENTAL SETTING DETAILS

Hyper-parameter	AlexNet	ResNet-18	DistilBERT
Activation function	ReLU	ReLU	None
Optimization method	SGD	SGD	SGD
Learning rate	0.01	0.01	0.01
Batch size	16	16	32
Data Distribution	IID and non-IID	IID and non-IID	IID
Global Epochs	200	200	80
Local Epochs	2	2	1
Learning rate decay	0.99 at each global Epoch	0.99 at each global Epoch	linear schedule with warmup
Client numbers	5,10, 20	5,10,20	5, 10, 20
Regularization Term	BCE loss, Hinge-like loss	BCE loss, Hinge-like loss	BCE loss, Hinge-like loss
α of Regularization Loss	0.2, 0.5, 1, 5	0.2, 0.5, 1, 5	100
Feature-based watermark parameters \mathbf{W}	\mathbf{W}^k and \mathbf{W}_γ	\mathbf{W}_k and \mathbf{W}_γ	\mathbf{W}_γ
Trigger-based watermark type	Adversarial sample	Adversarial sample	\
Backdoor batch size	2	2	\

TABLE 1: Training parameters for Federated AlexNet_P and ResNet_P-18, respectively (\dagger the learning rate is scheduled as 0.01, 0.001 and 0.0001 between epochs [1-100], [101-150] and [151-200] respectively).

Layer name	Output size	Weight shape	Padding
Conv1	32×32	$64 \times 3 \times 5 \times 5$	2
MaxPool2d	16×16	2×2	
Conv2	16×16	$192 \times 64 \times 5 \times 5$	2
Maxpool2d	8×8	2×2	
Conv3	8×8	$384 \times 192 \times 3 \times 3$	1
Conv4	8×8	$256 \times 384 \times 3 \times 3$	1
Conv5	8×8	$256 \times 256 \times 3 \times 3$	1
MaxPool2d	4×4	2×2	
Linear	10	10×4096	

TABLE 2: Modified AlexNet Architecture (Only embed feature-based watermarks across Conv3, Conv4 and Conv5, thus $M = 896$)

Layer name	Output size	Weight shape	Padding
Conv1	32×32	$64 \times 3 \times 3 \times 3$	1
Res2	32×32	$64 \times 64 \times 3 \times 3$ $64 \times 64 \times 3 \times 3$	$\times 2$ 1
Res3	16×16	$128 \times 128 \times 3 \times 3$ $128 \times 128 \times 3 \times 3$	$\times 2$ 1
Res4	8×8	$256 \times 256 \times 3 \times 3$ $256 \times 256 \times 3 \times 3$	$\times 2$ 1
Res5	4×4	$512 \times 512 \times 3 \times 3$ $512 \times 512 \times 3 \times 3$	$\times 2$ 1
Pooling	1×1	4×4	
Linear	100	100×512	

TABLE 3: Modified ResNet-18 Architecture (Only embed feature-based watermarks across Res5 Block, thus $M = 2048$)

Layer name	Sublayer	Weight shape
Embedding	Word Embedding	30522×768
	Position Embedding	512×768
	LayerNorm	1×768
Encoder1	Self-Attention Layer	$768 \times 768 \times 4$
	LayerNorm	1×768
	Feed Forward	768×3072 3072×768
	LayerNorm	1×768
Encoder2	Self-Attention Layer	$768 \times 768 \times 4$
	LayerNorm	1×768
	Feed Forward	768×3072 3072×768
	LayerNorm	1×768
...
Encoder6	Self-Attention Layer	$768 \times 768 \times 4$
	LayerNorm	1×768
	Feed Forward	768×3072 3072×768
	LayerNorm	1×768
Preclassifier		768×768
Classifier		Classes \times 768

TABLE 4: Modified DistilBERT Architecture (Only embed feature-based watermarks across Encoder Block 4, 5, 6, thus $M = 2304$)

Hyper-parameter	Value
Optimization method	Projected Gradient Descent
Norm type	L2
Norm of noise	0.3
Learning rate	0.01
PGD Batch size	128
Targeted at Specific Labels	True
Iterations	80
Learning rate decay	None
Vanilla Classification model	CNN with three convolution layers

TABLE 5: Training parameters for Projected Gradient Descent Adversarial Training